

Topics in air quality in Germany and China: Up-scaling of greenhouse gas emissions and meteorological and source influences upon urban air quality

Klaus Schäfer^a, Jürgen Böttcher^b, Daniel Weymann^c, Caroline von der Heide^b, Wilhelmus H.M. Duijnisveld^d, Rong-rong Shen^a, Patrick Wagner^e,

Hong Ling^{a, f}, Josef Cyrys^g, Christoph Münkel^h, Stefan Norraⁱ, Stefanie Schaderⁱ, Jürgen Schnelle-Kreisl, Yuesi Wang^f, Stefan Emeis^a, Peter Suppan^a

^aKarlsruher Institut für Technologie (KIT), Institut für Meteorologie und Klimaforschung, Bereich Atmosphärische Umweltforschung (IMK-IFU), Garmisch-Partenkirchen, Germany

^bLeibniz University Hannover, Institute of Soil Science, Hannover, Germany

^cForschungszentrum Jülich GmbH, Agrosphere Institute (IBG-3), Terrestrial Biogeochemistry, Jülich, Germany

^dGerman Federal Institute for Geosciences and Natural Resources, Hannover, Germany

^eUniversität Duisburg-Essen (UDE), Fakultät für Biologie, Angewandte Klimatologie und Landschaftsökologie, Essen, Germany

^fChinese Academy of Sciences (CAS), Institute of Atmospheric Physics (IAP), State Key Laboratory of Atmospheric Boundary Layer Physics and Atmospheric Chemistry (LAPC), 100029, Beijing, P. R. China

^gHelmholtz Zentrum München, German Research Center for Environmental Health (HMGU), Institute of Epidemiology II (EPI), Neuherberg, Germany

^hVaisala GmbH, Hamburg, Germany

ⁱKarlsruhe Institute of Technology (KIT), Institute of Geography and Geoecology (IGG), Karlsruhe, Germany

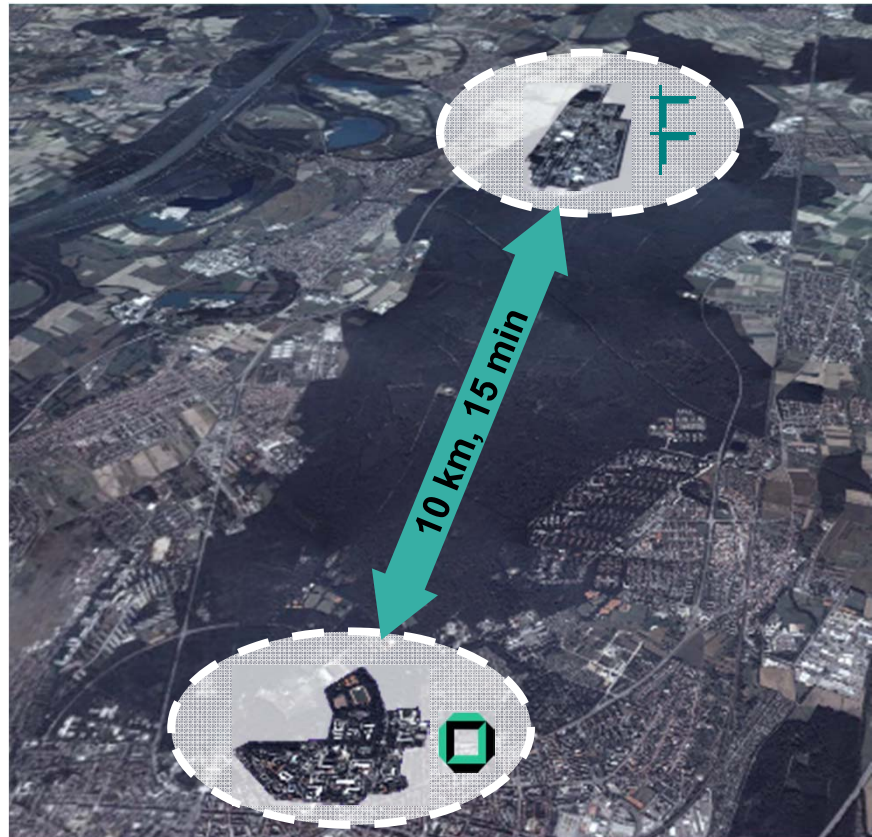
^jHelmholtz Zentrum München, German Research Center for Environmental Health (HMGU), Joint Mass Spectrometry Centre, Comprehensive Molecular Analytics, Neuherberg, Germany

INSTITUTE OF METEOROLOGY AND CLIMATE RESEARCH, DEPARTMENT ATMOSPHERIC ENVIRONMENTAL RESEARCH (IMK-IFU)



- Motivation, Objectives, Scientific questions
- Tasks, Methodology
- Results
- Conclusions

KIT Portfolio



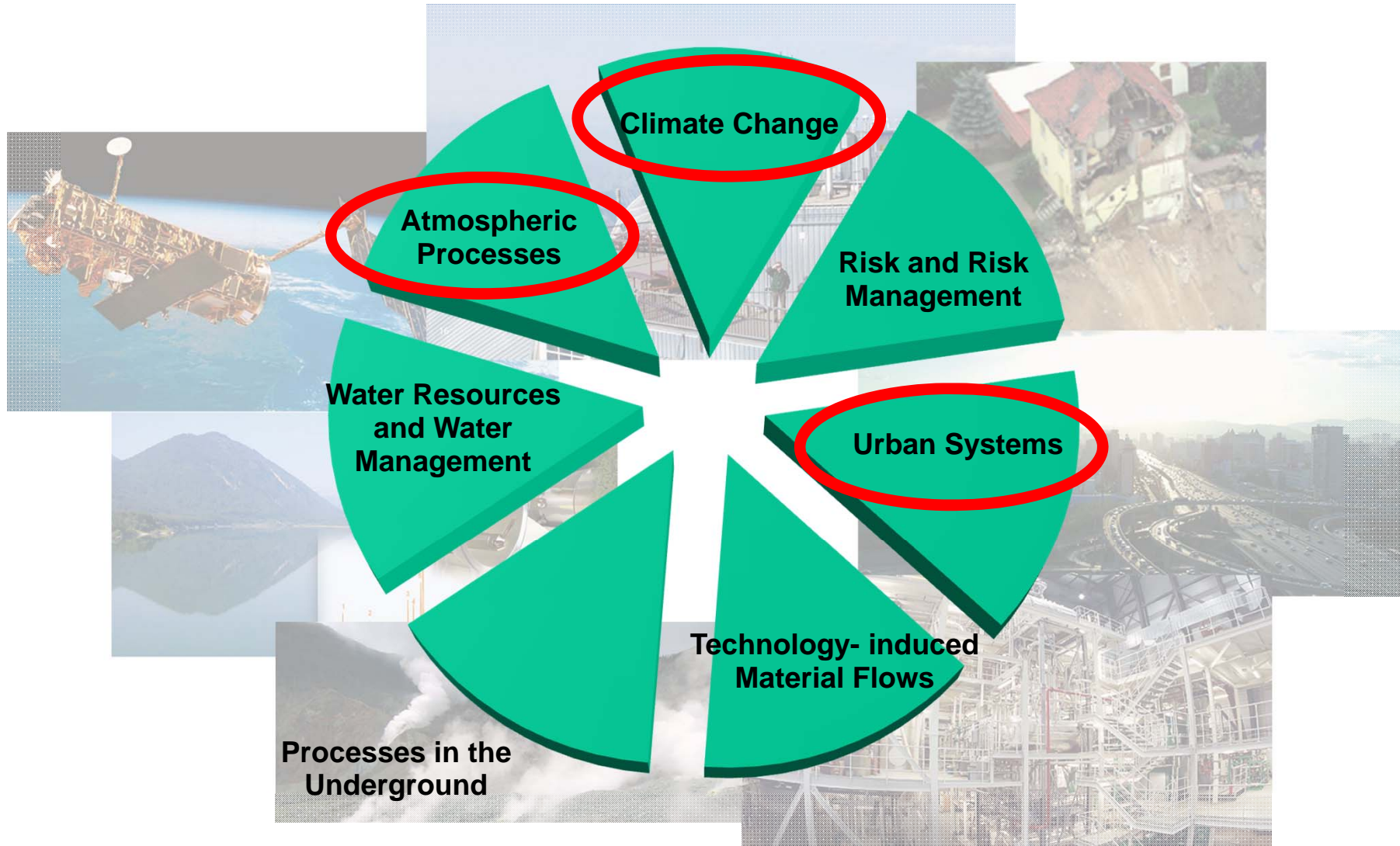
260 km



KIT - Centres

- Energy
- Climate and Environment
- Nano and Micro Scale Science
- Astroparticle Physics

KIT Center Climate and Environment

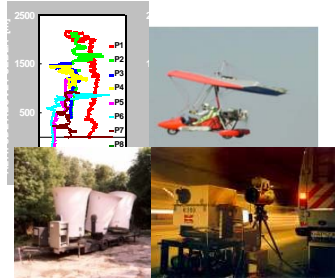


Integrated Approach

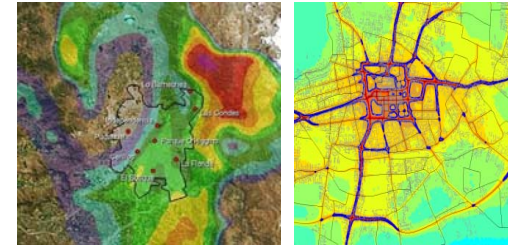
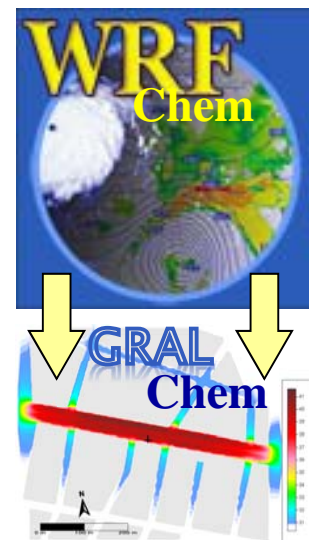
Urban Development



Measurement Data



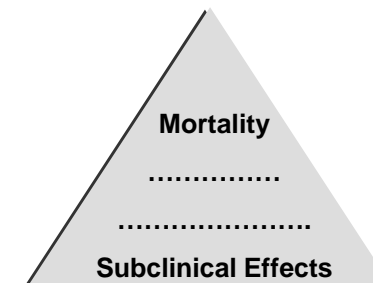
Traffic Data



Air Quality

Scenario

Indicator



Health Impact



Stakeholder

Source: Peter Suppan, KIT

Relevant strategic topics of the working group



“Regional coupling of ecosystem - atmosphere coupling”

- Knowledge about the interaction of coupled ecosystem – atmosphere processes within a changing climate
- Aerosol research (fine / ultra-fine particles) – loads / composition / formation / sources
- Coupling between urban air quality and regional climate change
- Process studies of air pollution relevant for health protection and legislation (NO_2 , PM_{10} , $\text{PM}_{2.5}$)

Up-scaling of greenhouse gas emissions

Background & Objectives



Up-scaling GHG emission measurements:

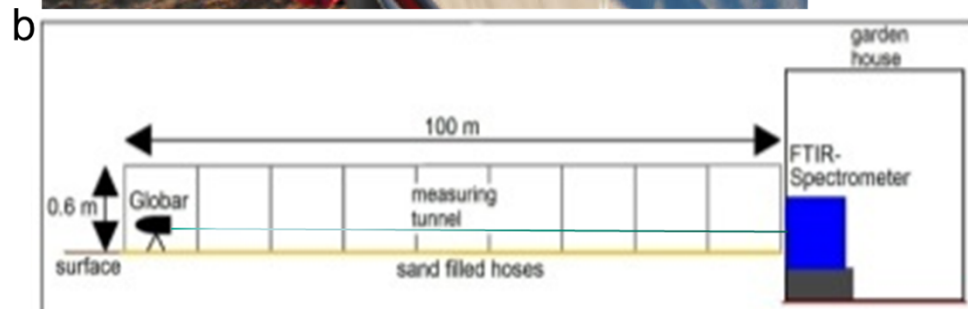
Micrometeorological techniques often limited by stable atmospheric conditions and their low spatial resolution

Closed tunnel on an area of 500 m² equipped with an open-path Fourier Transform Infrared (FTIR) spectrometer:

- (i) evaluate its feasibility for measuring N₂O concentrations and to calculate field-scale N₂O fluxes;
- (ii) compare those results with small-scale fluxes obtained from closed chamber measurements.

Tunnel experiment, chambers and flux calculation

- Measuring plot: unfertilized grassland on Gleyic Podzol in Northern Germany
- Tunnel: Aluminium liner structure ($99\text{ m} \times 5\text{ m} \times 0.6\text{ m}$), closed with a plastic cover for emission measurements; N_2O concentration measurements by path-averaged Fourier transform infrared (FTIR) spectrometry



The tunnel (a) with its dimensions and the FTIR unit (b), and the closed chambers (c) located at the same plot.

Methodology

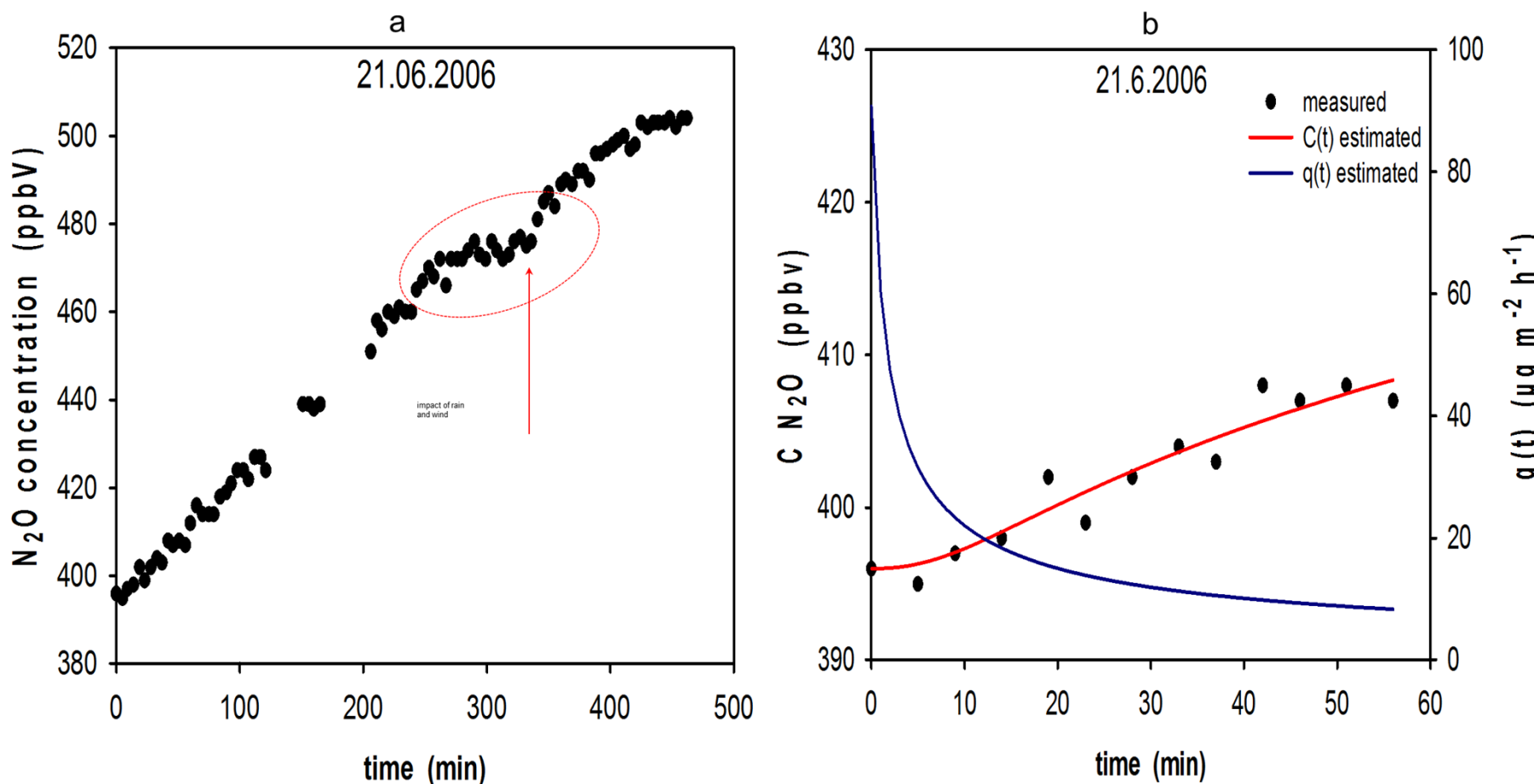
Calculation of a predeployment N_2O flux Q_0 by inverse modelling (IMQ0 model): 1D numerical model which takes into account specific tunnel geometry, N_2O diffusion from soil into the tunnel, N_2O diffusion within the tunnel atmosphere, N_2O detection by FTIR in 0.3 m above ground, and the diameter of the radiation beam (0.1 m)

Concurrent small-scale (0.05 m^2) chamber measurements; calculation of N_2O fluxes from four concentration measurements using the NDDE model (Livingston et al., 2006)

Results

Combined tunnel / FTIR method enables precise, high-density concentration measurements (about 12 per hr) during stable atmospheric conditions

Measurements are biased by high wind speeds, heavy rain and sun radiation



Representative time course of N₂O concentrations during a single measuring campaign (a) and measured concentrations during the first measuring hour with inversely estimated N₂O concentrations c_{N₂O} and N₂O flux q(t) (b).

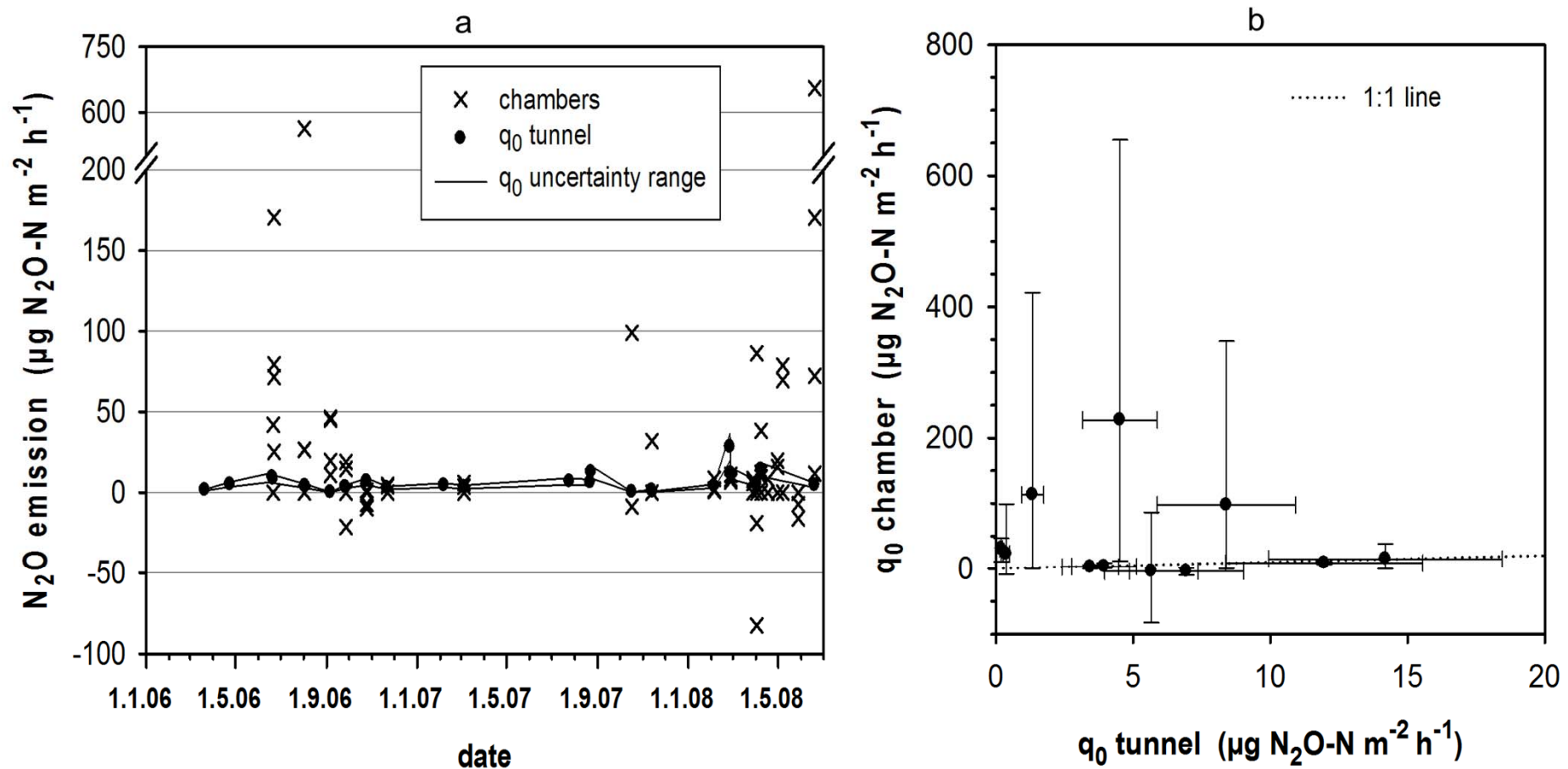
Results

Reliability of the IMQ0 model was confirmed using site-specific „virtual emission scenarios“ (Schäfer et al., 2012)

IMQ0 flux estimation was successfully applied to the experimental data

N_2O fluxes measured by the tunnel were small at a typical positive background level, whereas chamber-derived fluxes partly exhibited huge variability and slight N_2O uptake

High emissions obtained by single chambers occurred after rainfall events, but this hot spot behaviour was obviously not representative for the field or tunnel scale



Comparison of N_2O fluxes q_0 obtained by the small-scale chamber and field-scale tunnel methods.

Conclusions

N_2O concentration measurements with the tunnel / FTIR set up are reliable, particularly during dry and stable nocturnal conditions

IMQ0 model predicts the unbiased, pre-deployment N_2O flux with good accuracy

Field-scale tunnel method may serve as a gap-filling technique between small-scale chamber and ecosystem-level micrometeorological methods

Determination of meteorological parameters to study influences upon urban air quality

Motivation

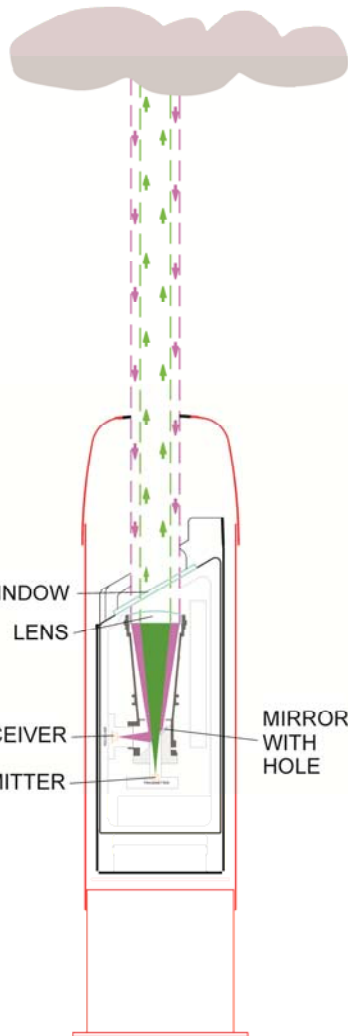


- Local emissions only cannot explain high air pollution episodes in urban areas, especially during cold seasons
- Detailed understanding of emission and chemistry/transport processes, directing certain air pollutant concentrations, not complete – but required for development of emission reduction measures
- Application of source apportionment methods needed
- Mixing layer height (MLH) controls the vertical space for rapid mixing of near-surface pollutants - essential for air quality forecast; influenced by climate change - quality of living in cities

Schäfer, K., Emeis, S., Hoffmann, H., Jahn, C.: Influence of mixing layer height upon air pollution in urban and sub-urban area. Meteorol. Z. 15 (2006), 647-658.

Methodology

CL 31 and 51 ceilometer



Typical range resolution for boundary layer

10 m

Backscatter profile range

Up to 15000 m

Range for boundary layer profiling

Up to 4000 m

Laser wavelength

910 nm



One-lens design – complete overlapping (Vaisala)

Continuous monitoring by uninterrupted remote sensing

Gradient method for MLH determination

Emeis, S., Schäfer, K.: Remote sensing method to investigate boundary-layer structures relevant to air pollution. *Bound-Lay. Meteorol.* 121, 377 (2006).

Methodology

Radio-acoustic Sounding System (RASS)

- profiles of wind speed,
 - wind direction, variance
 - of vertical wind component
 - and of acoustic temperature
- vertical resolution of 20 m
- up to a height of $h_{\max,R} = 540 \text{ m}$
- threshold of temperature gradient set at 1.0 K/100 m
- all values higher than this threshold taken as range of the upper boundary height of the detected layer ΔH

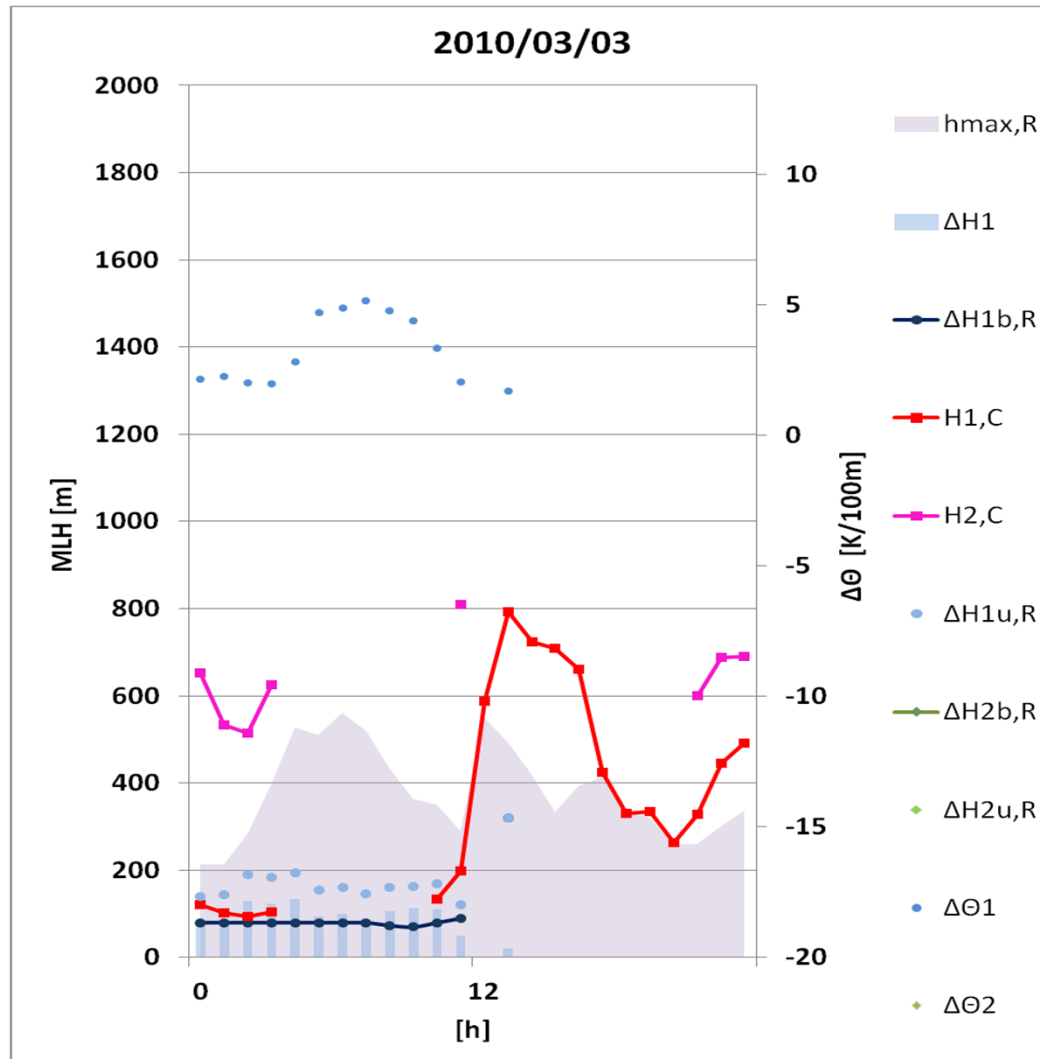


Methodology



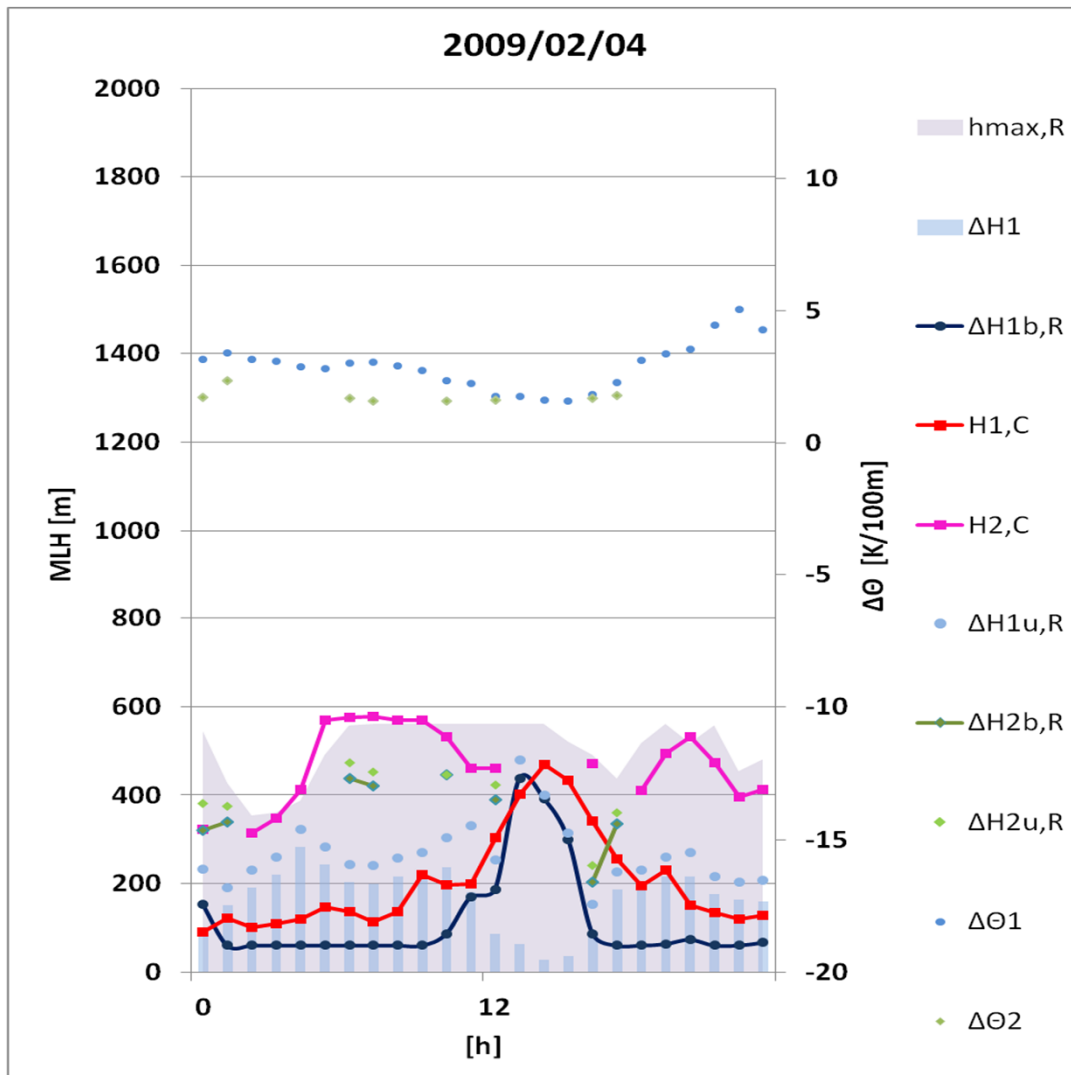
- Intercomparison for first and second detected layer above ground by RASS and ceilometer
- Only analyses of profile of temperature gradient from RASS measurements enables
 - an information about stability of layer and of depth of upper boundary of detected layer ΔH_1 or ΔH_2 ,
 - minimum of upper boundary height (lower most height of temperature gradient threshold exceedence) $\Delta H_{1b,R}$ or $\Delta H_{2b,R}$ and
 - a maximum of upper boundary height (upper most height of temperature gradient exceedence) $\Delta H_{1u,R}$ or $\Delta H_{2u,R}$

Ceilometer and RASS measurements in agreement

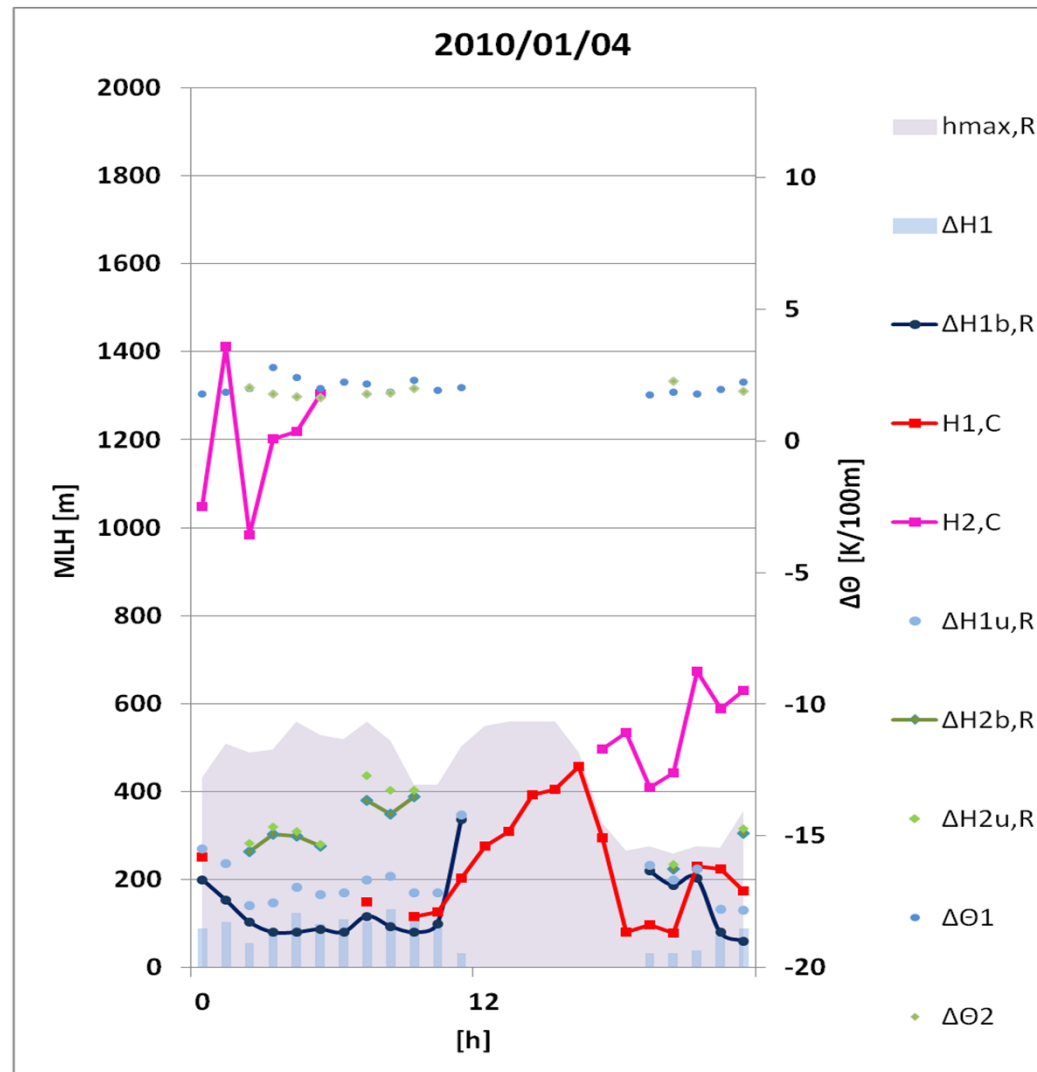


Ceilometer and RASS measurements

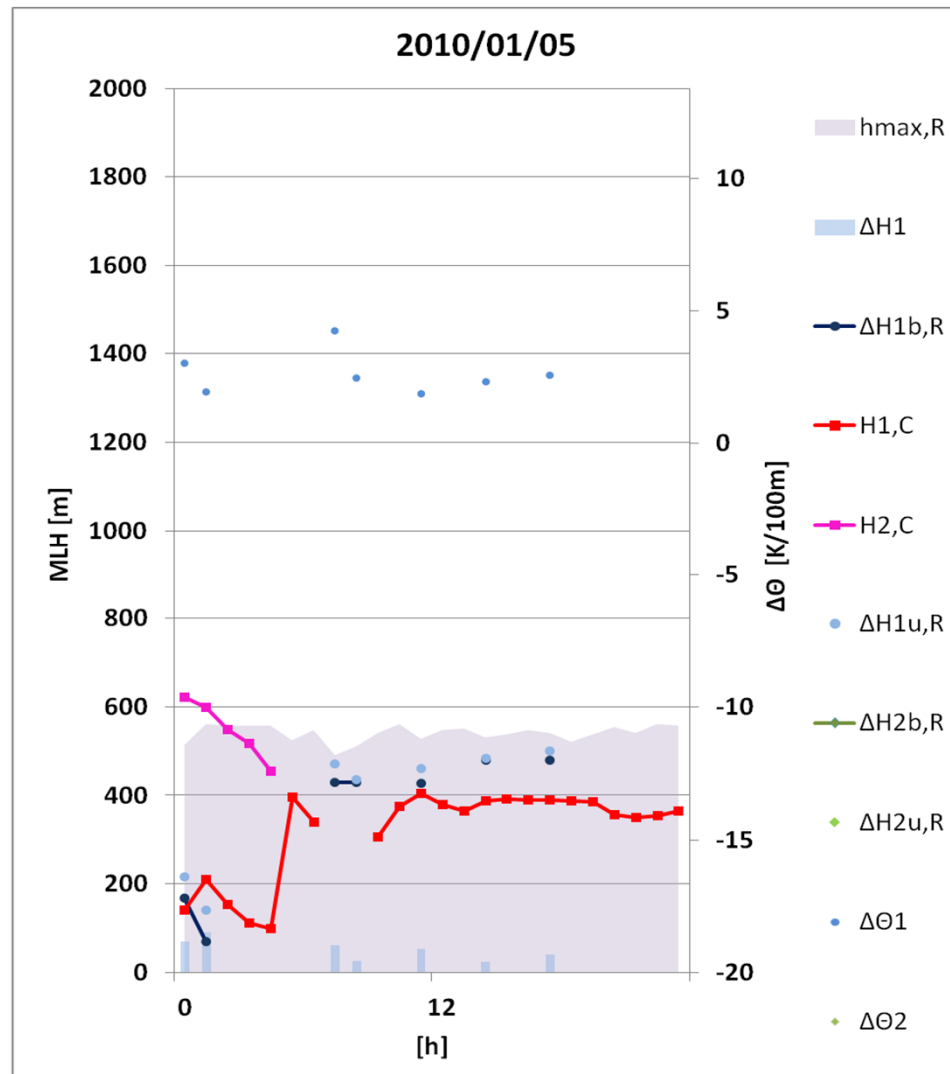
Information about thickness of atmospheric layers



Ceilometer and RASS measurements complete each other



Ceilometer and RASS measurements without realistic layer information



Conclusions



- Particle size spectrum influences ceilometer data in a non-quantifiable way
- Atmospheric humidity influences ceilometer data in a non-quantifiable way
- ➔ Ceilometers quite simple and return only one variable, optical backscatter intensity, their output needs careful analysis
- In late afternoon near-surface layer developed and a residual, second layer remaining sometimes but algorithms provide a down going upper boundary of first layer and a new second layer
- Fog and rain limit the capabilities of these remote sensing systems to detect layers

Conclusions



- If vertical temperature gradient not exceeding threshold value RASS cannot detect upper boundary of layers
- Strong winds reduce vertical variations of temperature and particle number density and thus limit remote sensing of both systems
- Depth of upper boundary of detected layers provided by RASS important information about layering characteristics
- If information about upper boundary of layers during daily course interrupted continuity of data must be checked because of rapid changes of layering during front passages

Emeis, S., Schäfer, K., Münkel, C.: Observation of the structure of the urban boundary layer with different ceilometers and validation by RASS data. Meteorologische Zeitschrift 18, 2, 149-154 (2009); DOI: 10.1127/0941-2948/2009/0365.

Meteorological influences upon urban air quality

Particle size distribution

Objectives



- Influences of meteorological parameters and atmospheric layering (especially mixing layer height (MLH)) on exchange processes of ground level emissions
- Application of ceilometer monitoring information for MLH to interpret air pollution near ground
- Measurements in Augsburg at urban background site (particle size distributions) and kerb site (NO , NO_2 , O_3) and in Essen at kerb site (Benzene, Toluene, Isoprene, NO , NO_2 , PM_{10})
- Strongest MLH influence: hourly-mean or maximum values

Schäfer, K., Emeis, S., Hoffmann, H., Jahn, C.: Influence of mixing layer height upon air pollution in urban and sub-urban area. Meteorol. Z. 15, 647 (2006).

Tasks in Augsburg



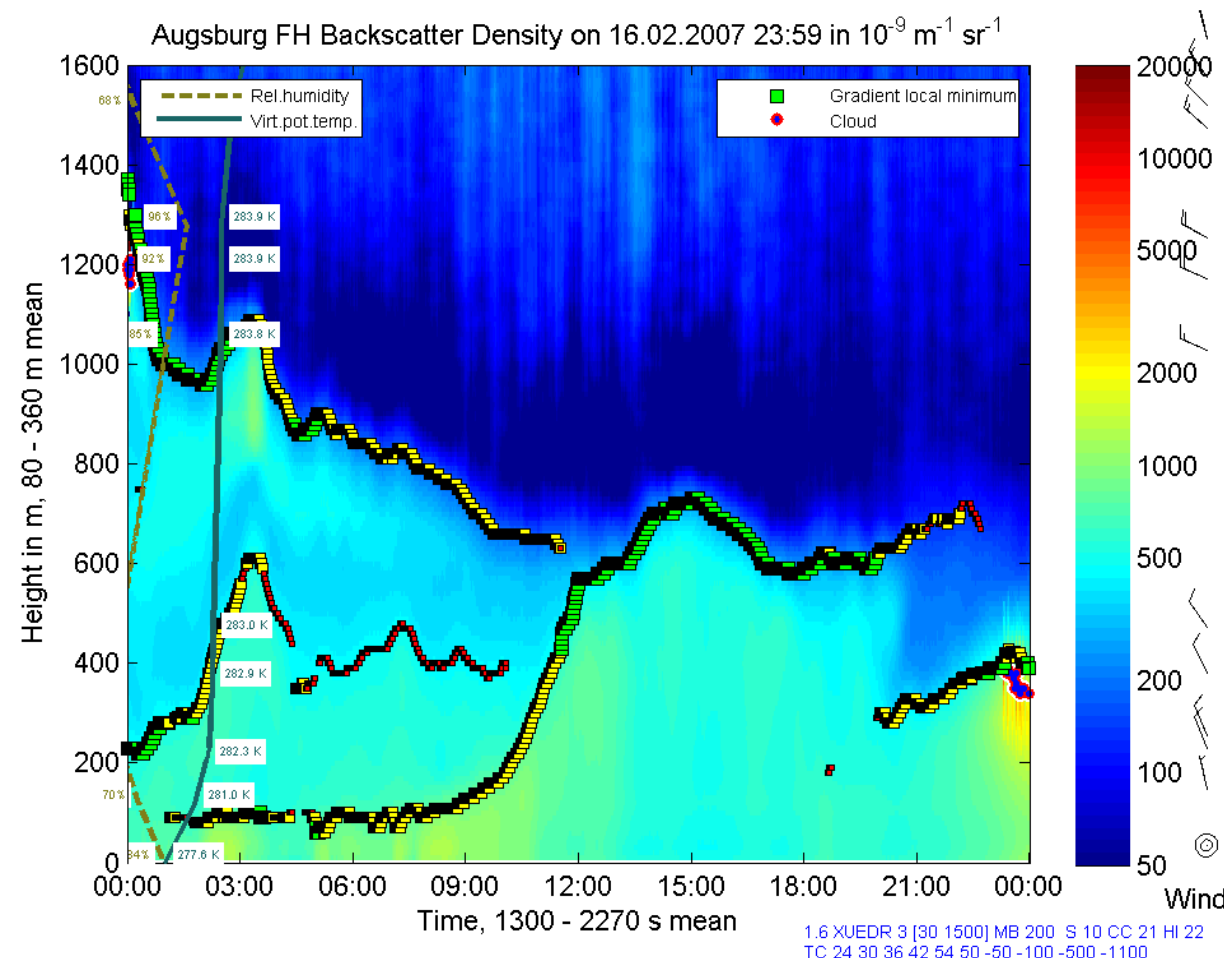
Measurements of meteorological parameters and air pollutant concentrations: 16-23/02/2007, 14-23/02/2008

- MLH: Measured by CL31 (*IMK-IFU*), software developed with MATLAB (*Vaisala, IMK-IFU*); radiosondes *DWD* station Oberschleissheim
- Particle number concentrations (PNC) and mass concentrations (PMC): urban background site (*HMGU, EPI II; UA, WZU*)
- Meteorological parameters (*Lfu; DWD; HMGU, EPI II*)

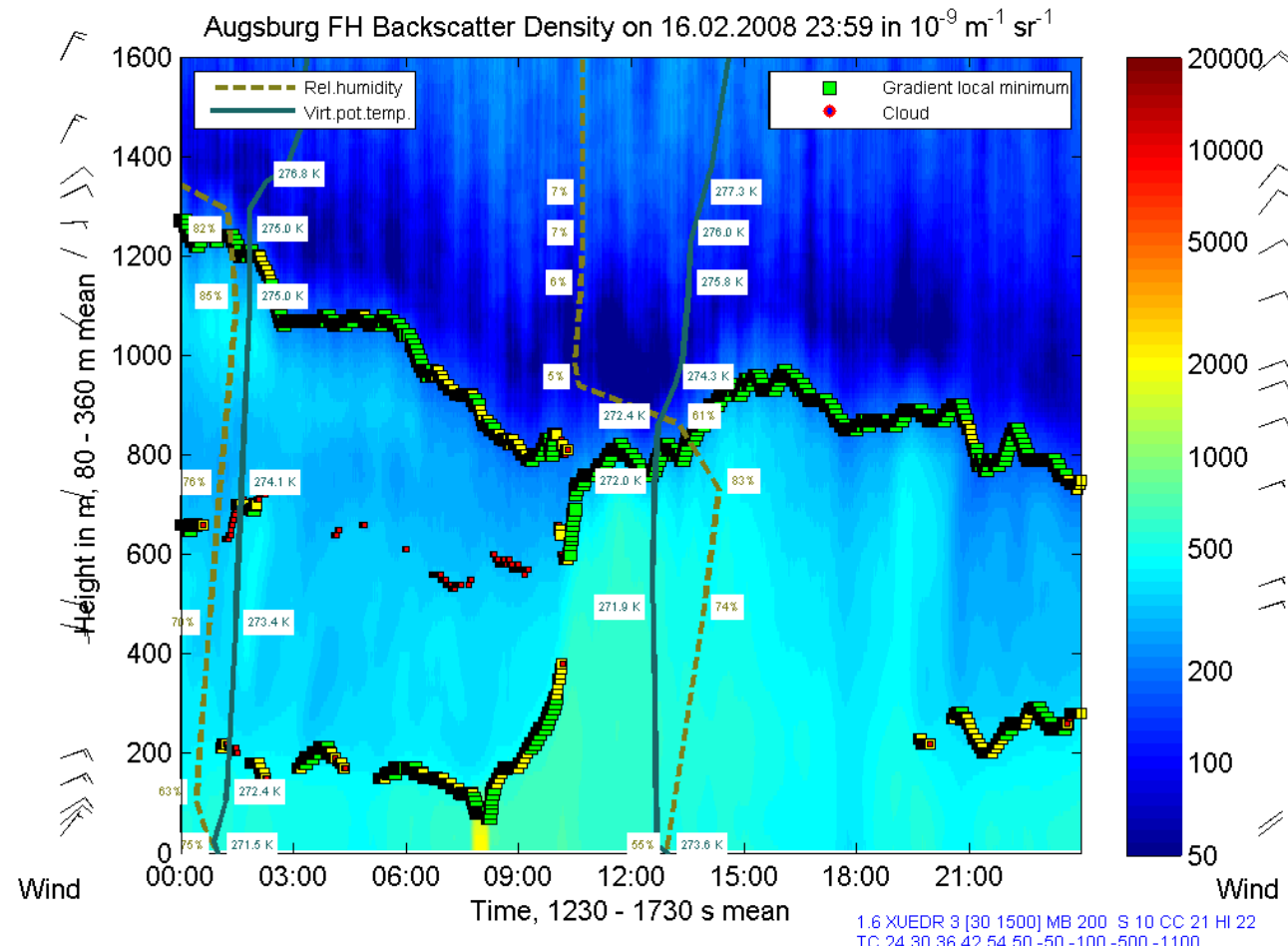
Correlations of continuous MLH, temperature, wind direction, wind speed and relative humidity data with PNC and PMC of different size fractions, hourly mean data (*IMK-IFU*)

Pitz, M., Birmili, W., Schmid, O., Peters, A., Wichmann, H.E., Cyrys, J.: Quality control and quality assurance for particle size distribution measurements at an urban monitoring station in Augsburg, Germany. *J. Environ. Mon.* 10(9), 1017-1024 (2008).

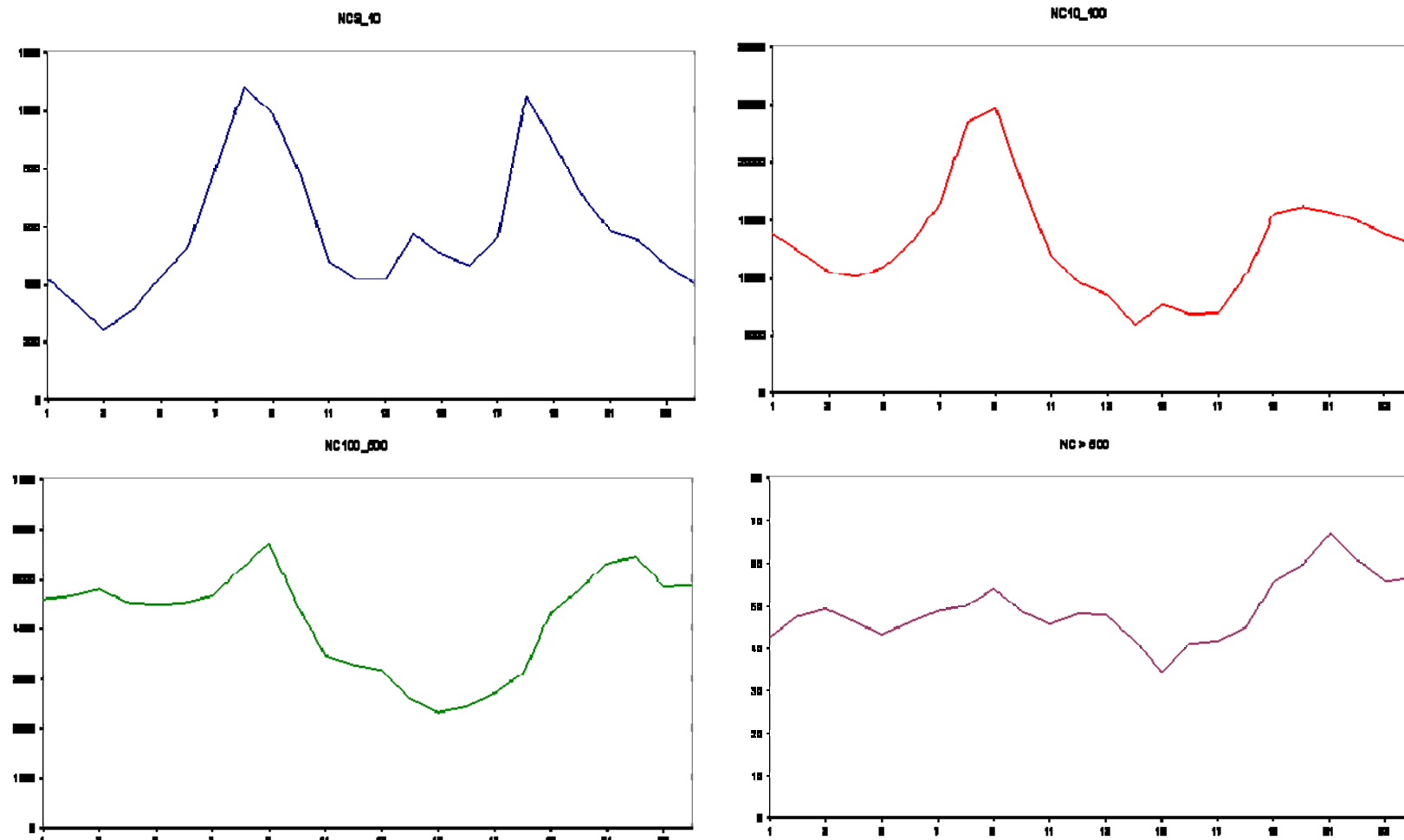
Ceilometer measurements in Augsburg Radiosonde measurements in Oberschleißheim (60 km distance)



Ceilometer measurements in Augsburg Radiosonde measurements in Oberschleißheim (60 km distance)



Ultra-fine particle measurements in Augsburg



Diurnal pattern of PNC 16-23/02/2007: 3-10 and 10-30 strong variation; 100-500 high night-time values; >500 weak variation

Spearman correlation coefficients R² of PNC, PMC with MLH and wind speed

hourly mean, significant >0.24: measurement errors 10 and 15 %

PNC		3 – 10	10 – 30	30 – 50	50 – 100	100 – 500	500 – 1000	1000 – 2500	2500 – 10000
2007	MLH	0.01	0.02	0.06	0.12	0.11	0.03	0.00	0.00
2008	MLH	0.00	0.15	0.24	0.35	0.46	0.19	0.16	0.07
2007	W speed	0.00	0.05	0.14	0.26	0.38	0.20	0.15	0.17
2008	W speed	0.01	0.11	0.23	0.35	0.42	0.10	0.11	0.19
PMC		3 – 10	10 – 30	30 – 50	50 – 100	100 – 500	500 – 1000	1000 – 2500	2500 – 10000
2007	MLH	0.01	0.03	0.07	0.13	0.07	0.02	0.00	0.00
2008	MLH	0.00	0.18	0.25	0.37	0.44	0.18	0.20	0.05
2007	W speed	0.00	0.08	0.19	0.39	0.44	0.22	0.18	0.12
2008	W speed	0.00	0.11	0.20	0.38	0.38	0.04	0.13	0.14

Daytime correlation coefficients smaller than during night-time

Conclusions

- Surface emissions - main sources of UFP in the atmosphere
 - Accumulation, coagulation and nucleation form very rapidly coarser particles
 - Larger particles (e.g. particle size range 500 - 1000 nm) influenced by formation of secondary particles
- MLH influence upon PMC significant also (as for $\text{PM}_{2.5}$, PM_{10})
 - 80 % of PNC represented by size fractions up to 100 nm
 - 70 % of PMC in size fraction 100 – 500 nm

Schäfer, K.; Emeis, S.; Schrader, S.; Török, S.; Alfoldy, B.; Osan, J.; Pitz, M.; Münkel, C.; Cyrys, J.; Peters, A.; Saragiannis, D.; Suppan, P.: A measurement based analysis of the spatial distribution, temporal variation and chemical composition of particulate matter in Munich and Augsburg. Meteorol. Z. 21, 1, 47-57 (2011)

Meteorological influences upon urban air quality

Traffic gaseous emissions in Augsburg

Tasks in Augsburg



Measurements March – September 2012

Path-integrated, in situ concentrations of NO, NO₂, O₃ at a crossing (*IMK-IFU*)

- diurnal variations
- influences from emissions, weather conditions, chemical / photochemical reactions

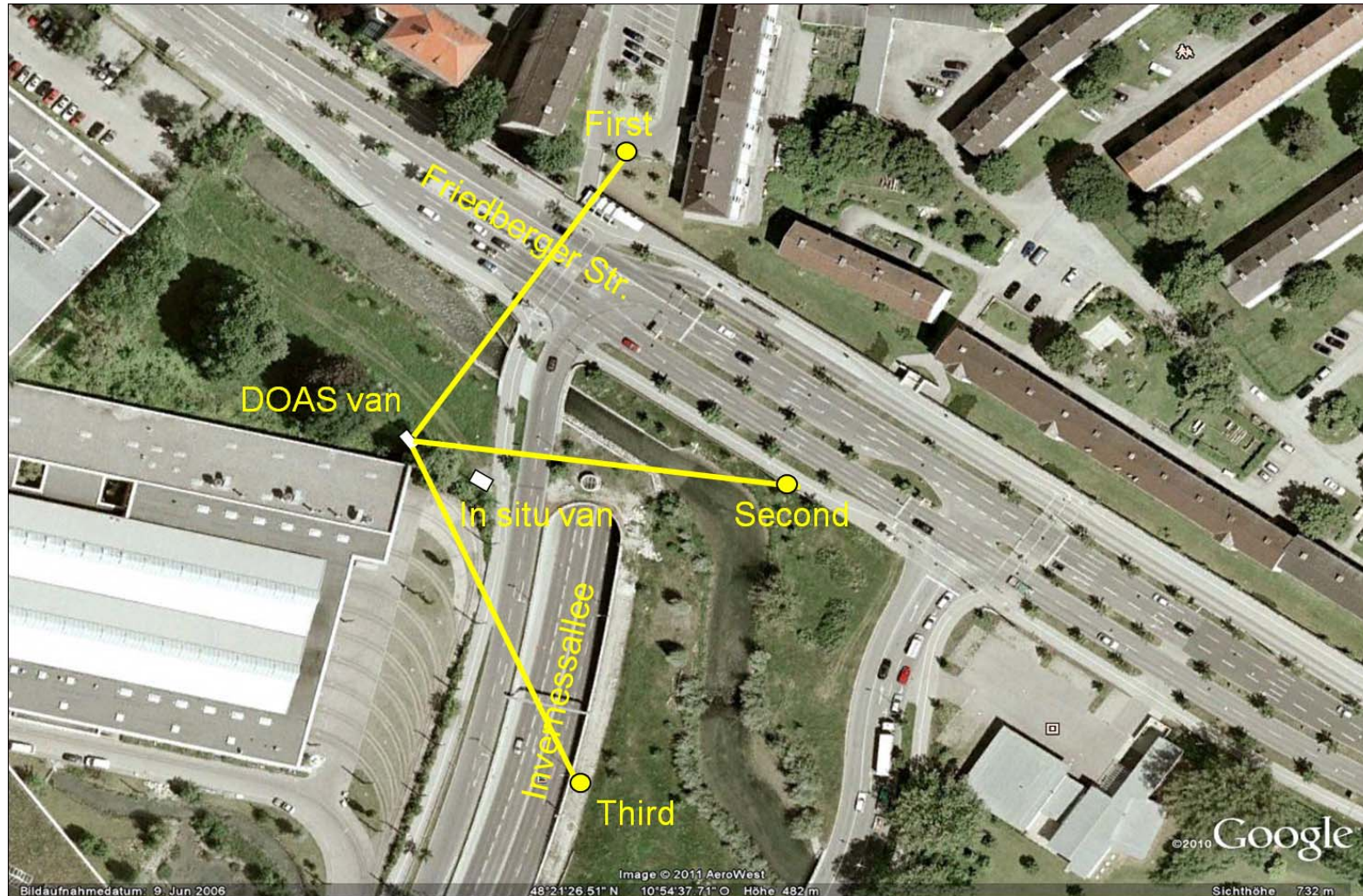
Correlations of continuous MLH, temperature, wind direction, wind speed and relative humidity data with air pollutant data

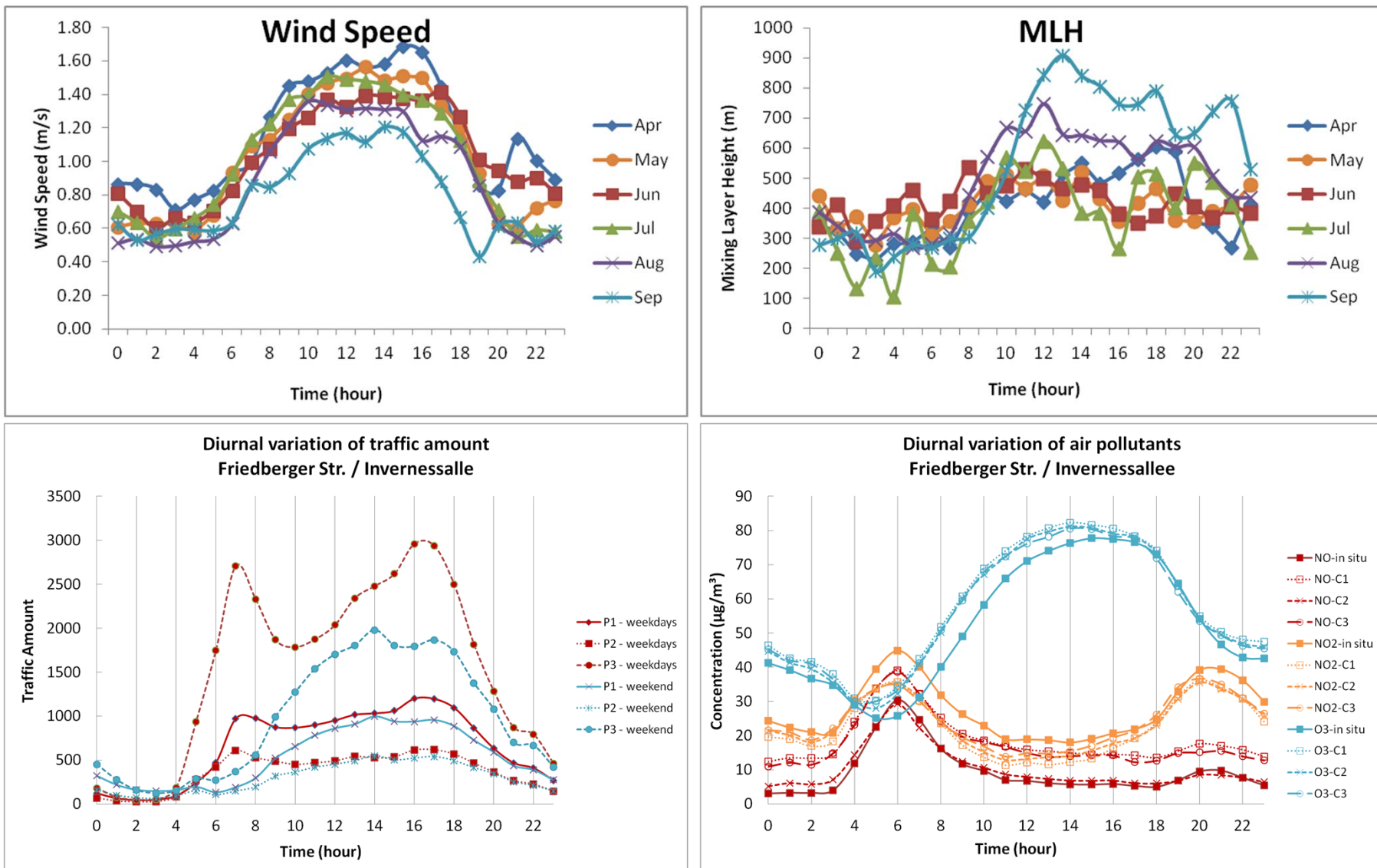
Schäfer, K., Emeis, S., Schrader, S., Török, S., Alföldy, B., Osan, J., Pitz, M., Münkel, C., Cyrys, J., Peters, A., Saragiannis, D., Suppan, P.: A measurement based analysis of the spatial distribution, temporal variation and chemical composition of particulate matter in Munich and Augsburg. Meteorol. Z., 21, 1, 47-57 (2011).

DOAS (Differential Optical Absorption Spectroscopy) instrument



Continuous DOAS measurements in Augsburg





Conclusions



- Path-integrated measurements by DOAS satisfy task of long-term and multiple-compound monitoring of traffic emissions better than in situ measurements
- Diurnal patterns of NO, NO₂ at kerb site caused by
 - traffic emissions mainly,
 - local convection,
 - chemical transformations
- A lot of effort required for quantitative determination of MLH

Meteorological influences upon urban air quality

Traffic gaseous emissions in Essen

Tasks in Essen



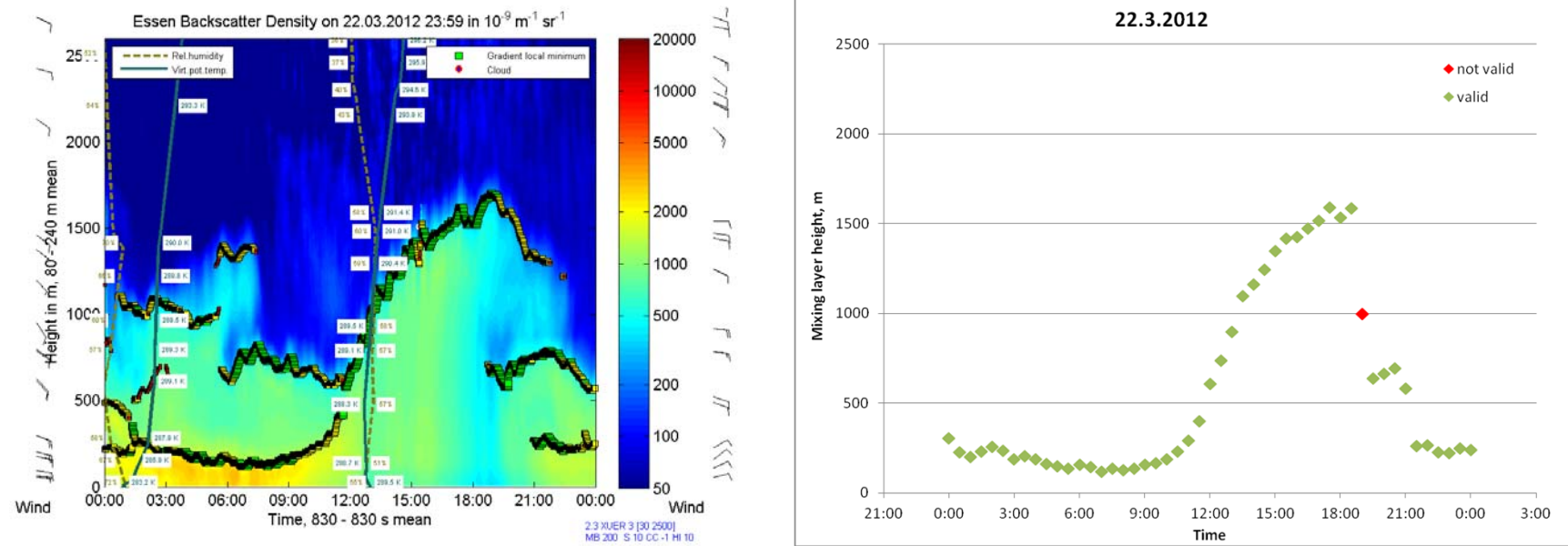
Measurements 28/12/2011-17/04/2012, VOC 28/02-03/04/2012

- Benzene, Toluene, Isoprene concentrations: every half hour by on-line gas-chromatograph GC955 from Synspec b.v., during 20 min enriched on Tenax GR, kerb site Gladbecker Str. (*UDE*)
- NO, NO₂ and PM₁₀ concentrations of LANUV Nordrhein-Westfalen: kerb site Gladbecker Str.

Correlations of continuous MLH with air pollutants (*UDE, IMK-IFU*)

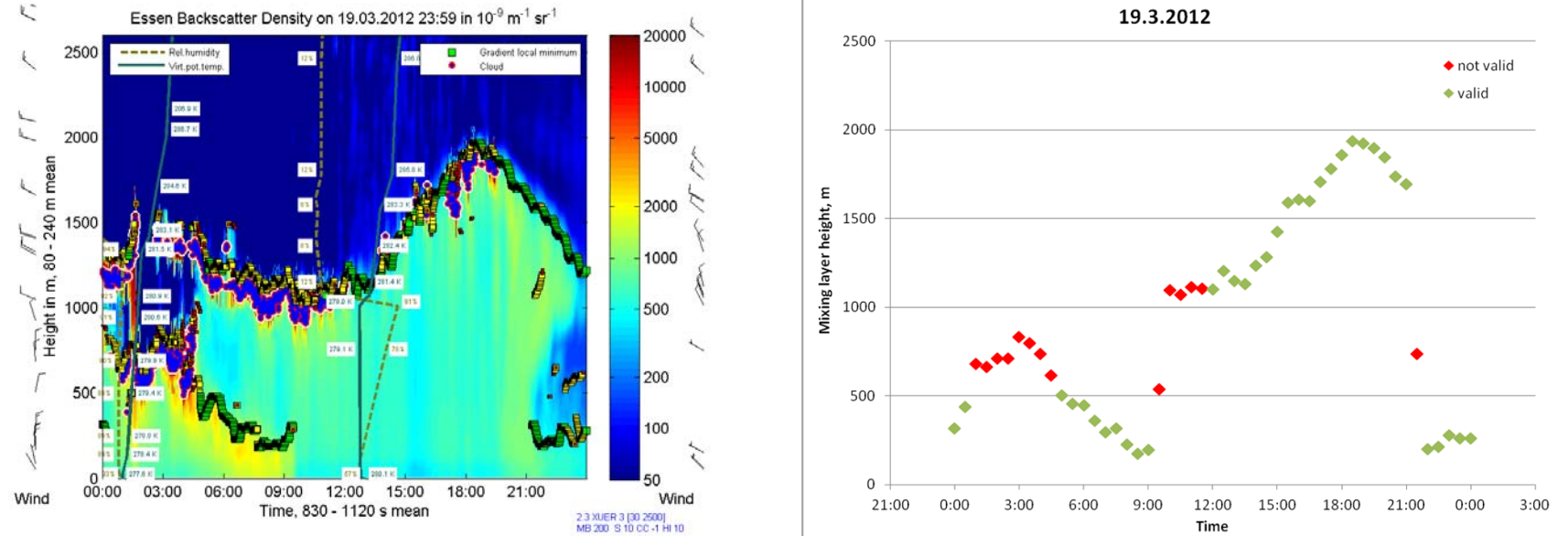
Wagner, P., Kuttler, W.: Biogenic and anthropogenic isoprene in the near-surface urban atmosphere - A case study in Essen, Germany. *Sci. Total Environ.*, 475, 104–115 (2014).

Ceilometer and radiosonde measurements



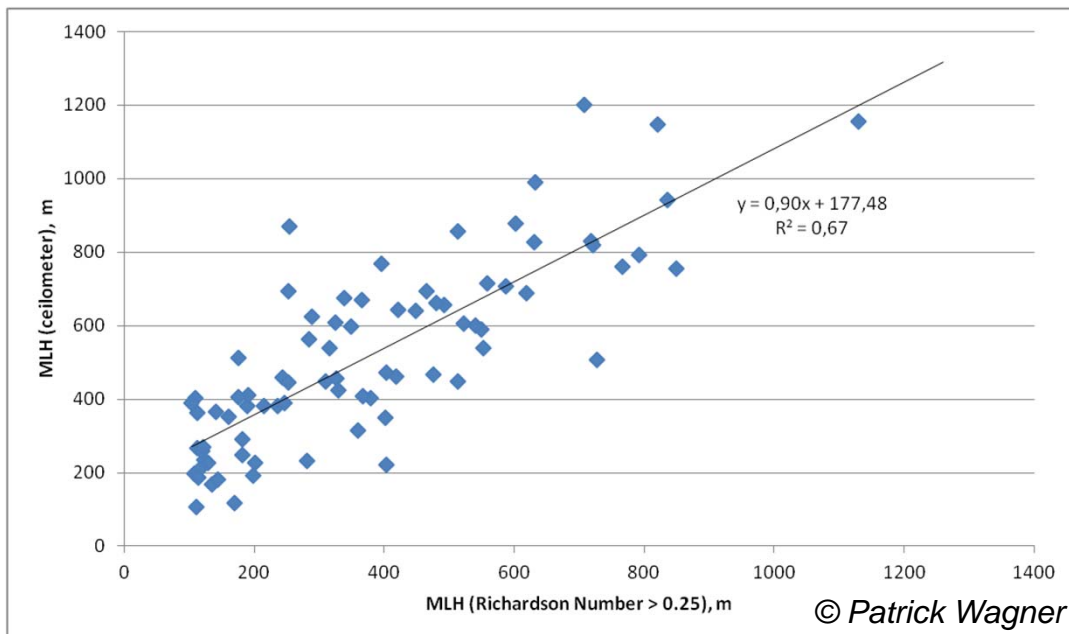
- Residual layer during late night
- Increasing MLH during day-time
- Formation of a near surface layer during evening

Ceilometer and radiosonde measurements



- Time frames with low clouds excluded
- Cloud upper boundary is layer upper boundary 17:00 - 20:00
- No time periods with high variability of MLH considered: abrupt rise due to solar heating, formation of nocturnal inversion

Comparison of mixing layer height measurements from ceilometer and radiosonde



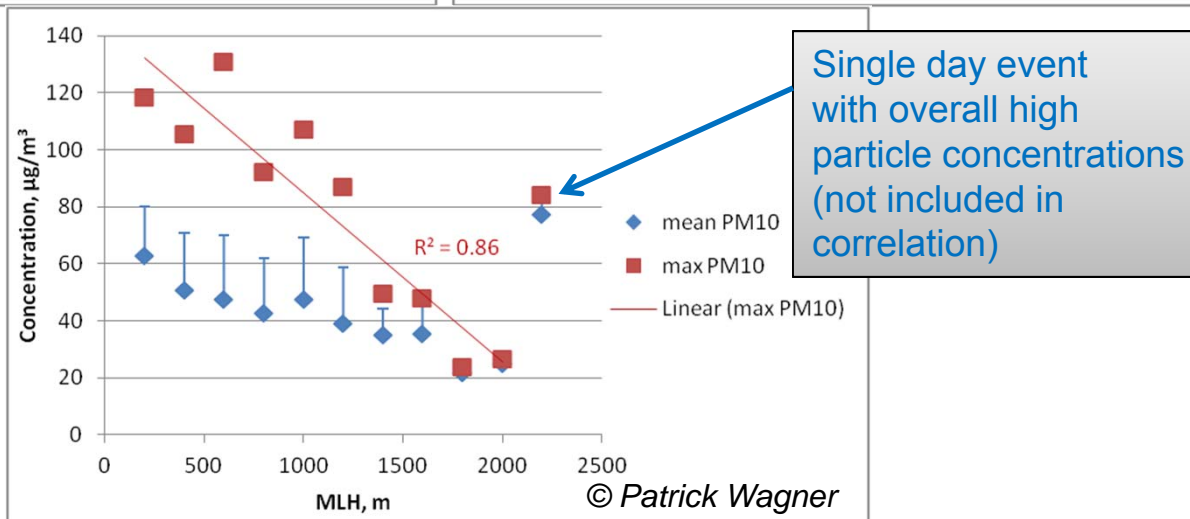
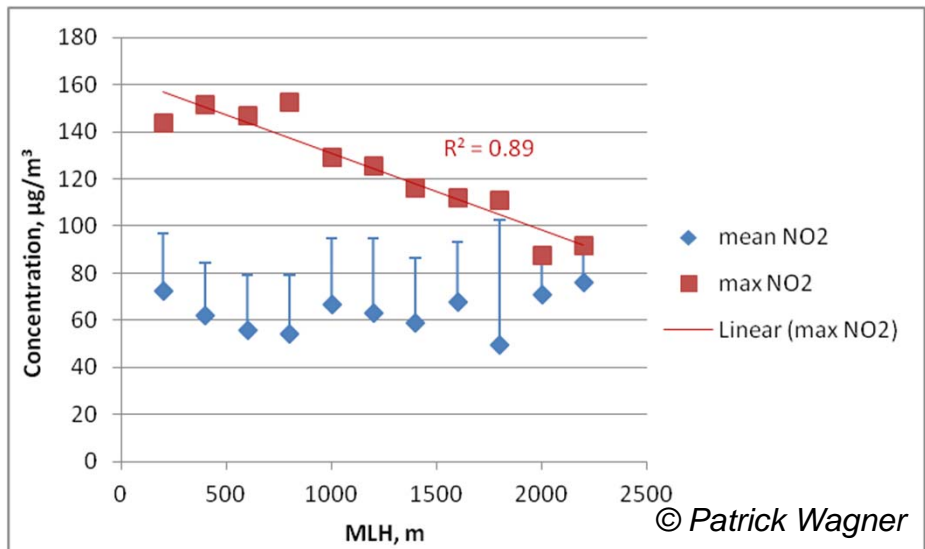
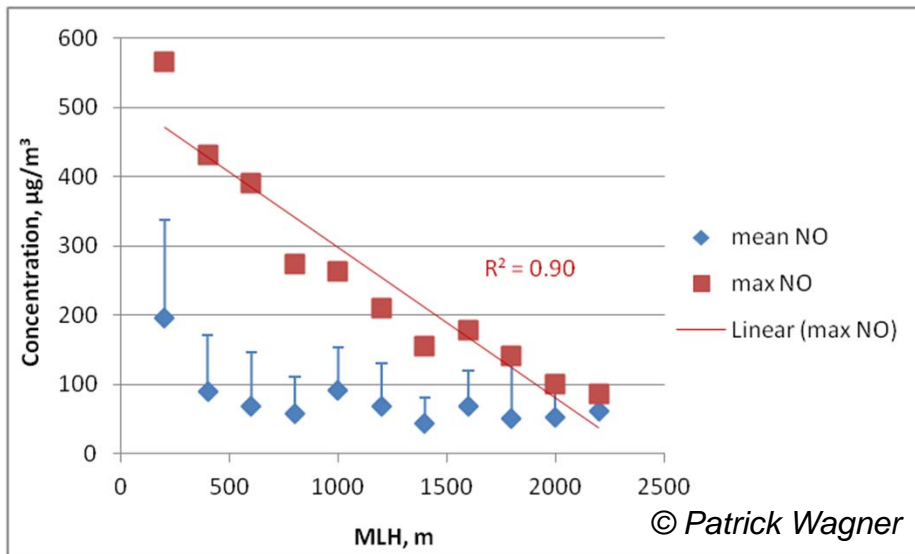
Deviations might be caused by:

1. Complex particle gradient structure affecting ceilometer MLH retrieval
2. Short-term stable layers affecting radiosonde measurements (threshold $Ri_c = 0.25$ used for MLH determination)
3. Urban heat island (city centre: ceilometer; suburban site: radiosonde)

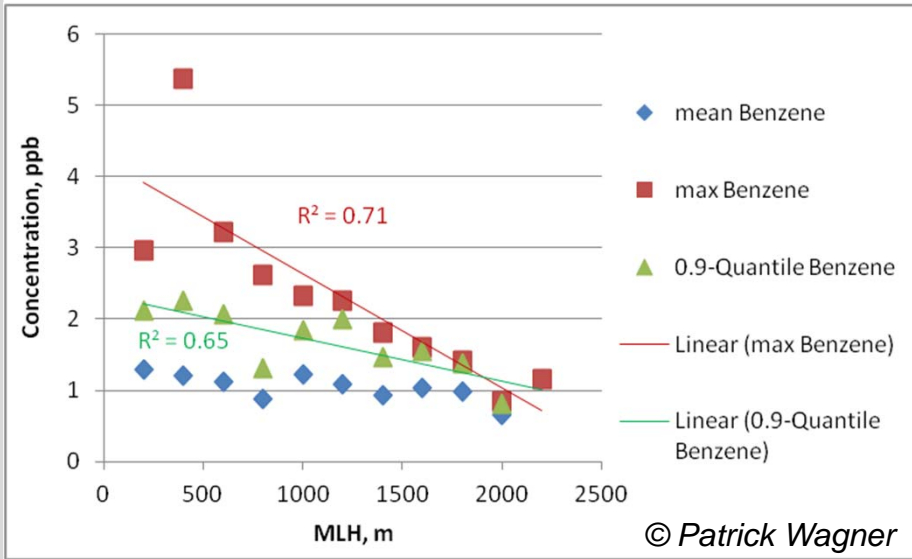
Methodology

- **MLH:** statistical classification scheme of Sturges:
 $K = 1 + 3.32 \log N$, K number of classes, N number of data
- 11 **classes** and a class width of **200 m intervals** of MLH
(200 m – 2200 m) instead of original 10 m intervals
- Mean and **maximum concentration** determined for each MLH class

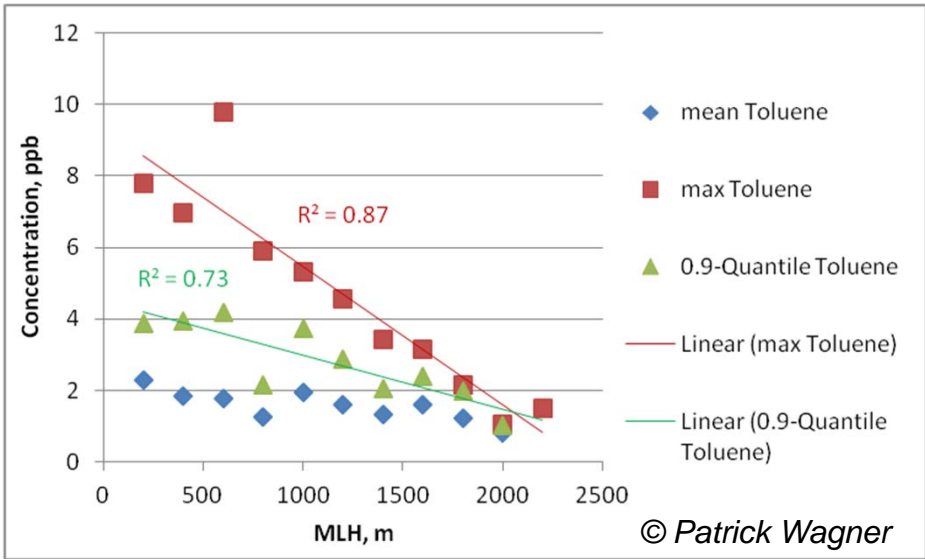
Correlations



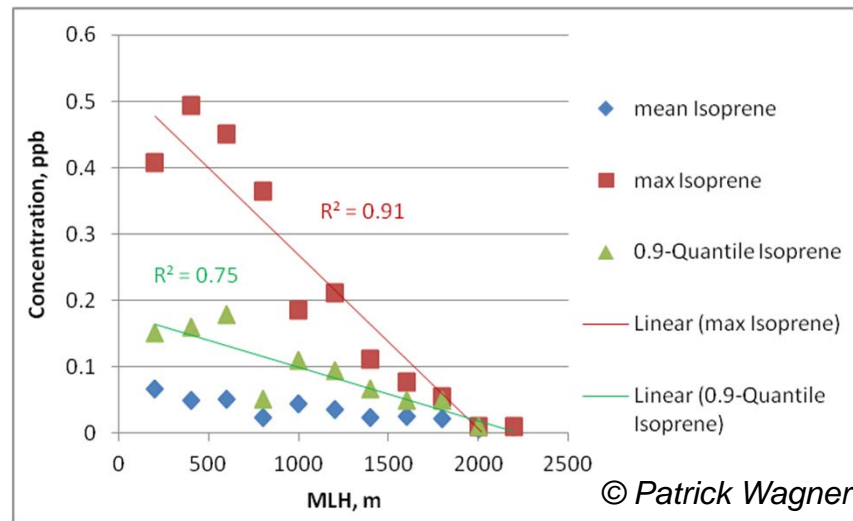
Correlations



© Patrick Wagner



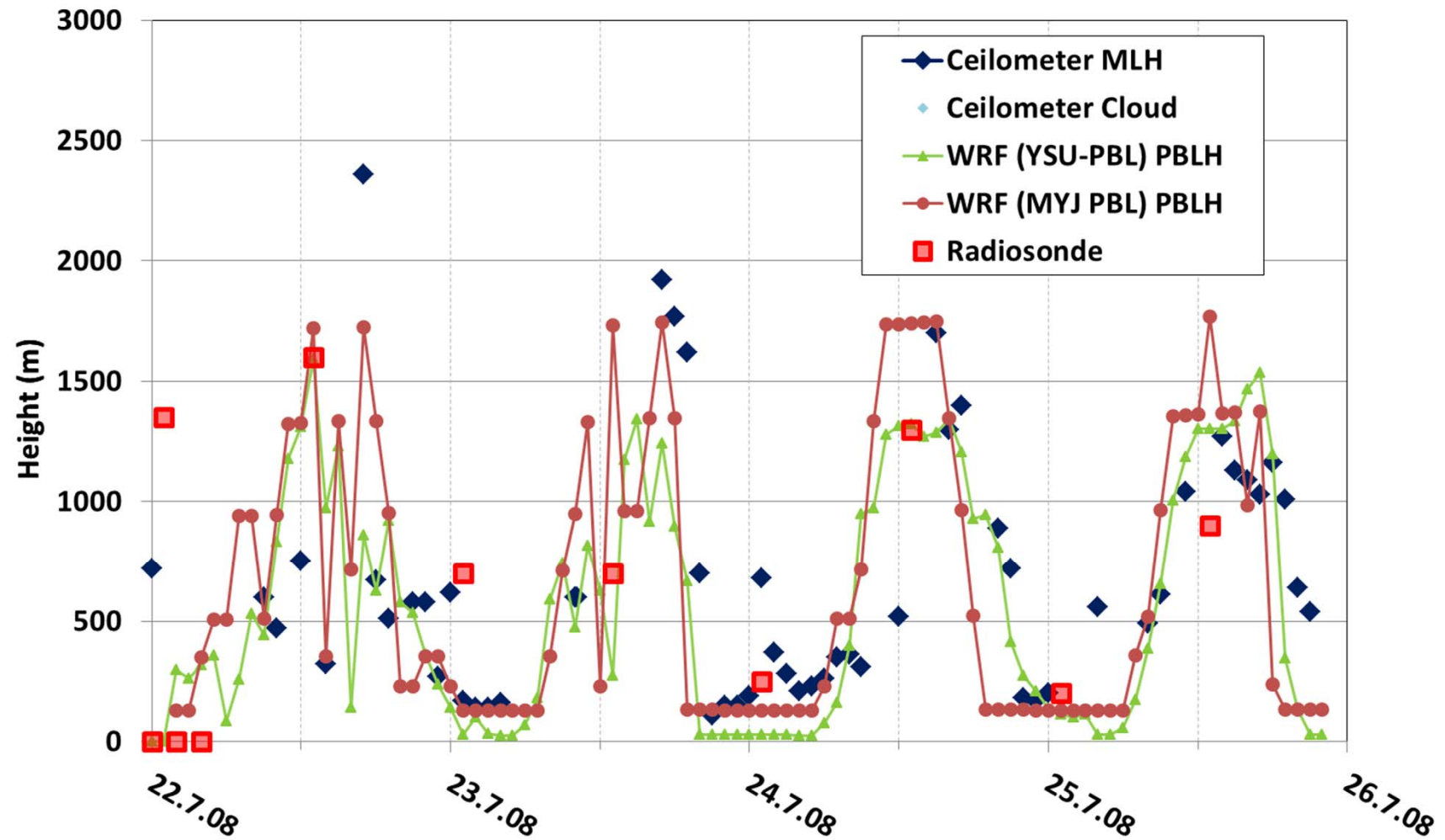
© Patrick Wagner



© Patrick Wagner

MLH comparison

ceilometer – modelling by WRF



Conclusions

- Maximum concentrations affected strongly by MLH and atmospheric stability
- Best correlation results for 200 m intervals of MLH
- Higher correlation coefficients of maximum NO, NO₂, PM₁₀, Benzene, Toluene, Isoprene concentrations in street canyon with MLH than for mean concentrations in urban and rural background with MLH (Munich, Hannover, Augsburg, Budapest, Athens)

Alföldy, B., Osán, J., Tóth, Z., Török, S., Harbusch, A., Jahn, C., Emeis, S.; Schäfer, K.: Aerosol optical depth, aerosol composition and air pollution during summer and winter conditions in Budapest. *Sci. Total Environ.*, 383, 141-163, (2007).

Schnelle-Kreis, J., Orasche, J., Abbaszade, G., Schäfer, K., Harlos, D.P., Hansen, A.D.A., Zimmermann, R.: Application of direct thermal desorption gas chromatography time-of-flight mass spectrometry for determination of non-polar organics in low volume samples from ambient particulate matter and personal samplers. *Anal. Bioanal. Chem.*, 401, 3083–3094 (2011).

Helmis, C. G., Sgouros, G., Flocas, H., Schäfer, K., Jahn, C., Hoffmann, M., Heyder, C., Kurtenbach, R., Niedojadlo, A., Wiesen, P., O'Connor, M., Anamaterou, E.: The role of meteorology on the background air quality at the Athens International Airport. *Atmos. Environ.*, 45, 5561-5571 (2011).

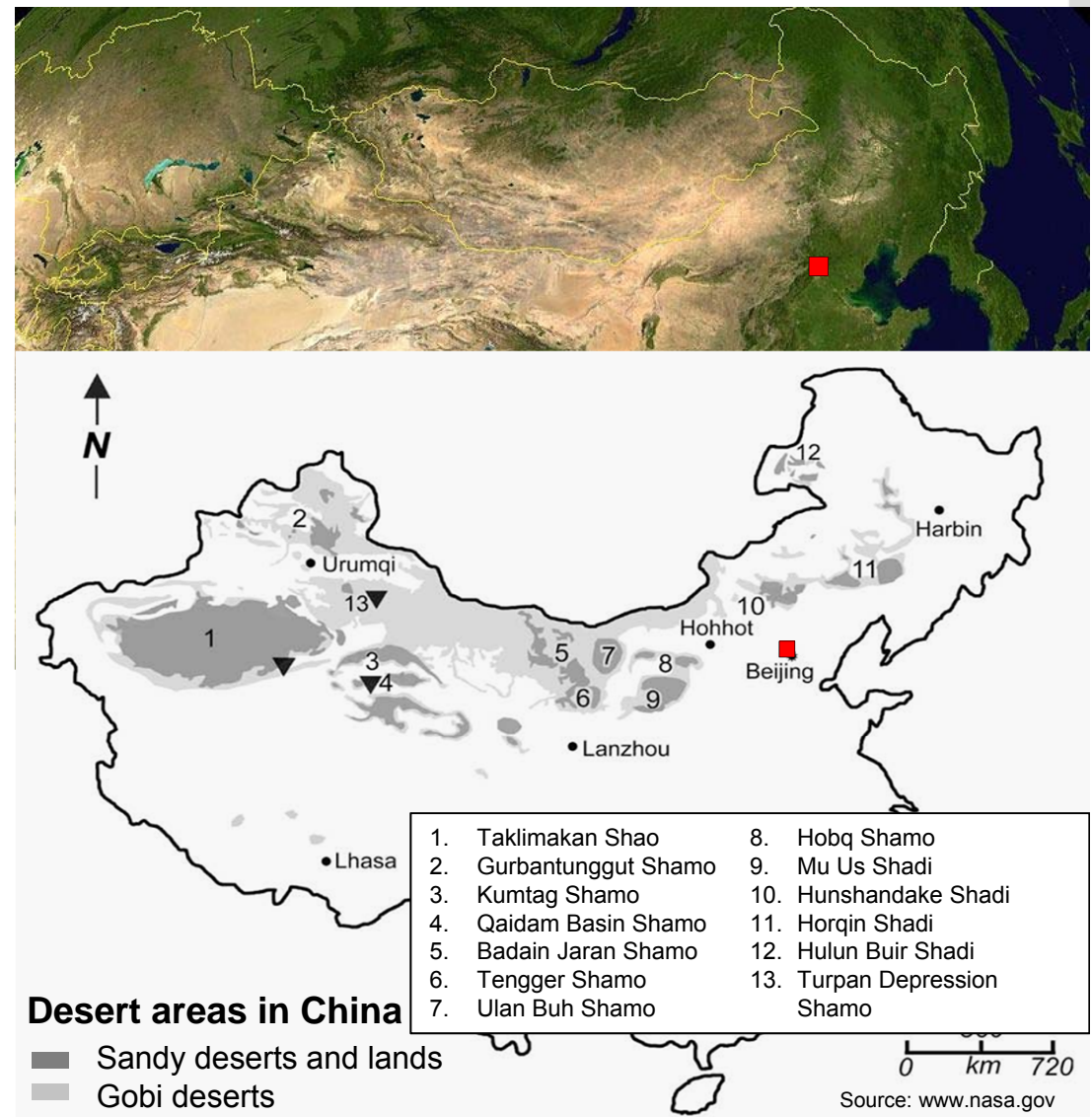
Meteorological influences upon urban air quality

Anthropogenic air pollutant exposure in Beijing

Tasks in Beijing

Aeolian mineral dust originated from West and Northwest during storm events – can carry pollutants and nutrients

Emission reduction measures to improve air quality during the Olympic Summer Games in 2008: cut down coarse particles mainly, still frequent air pollution events



Source apportionment for air quality

- Local and regional wind systems - can bring fresh air masses or polluted air flow: westerly or southerly wind directions
- Role of orography – mountains in the West to Northeast
- Role of industrial areas – in the South
- Heat island effect



Methodology

tower: meteorology, air quality; DOAS 04/09 – 03/11: NO₂, NO, SO₂, O₃, NH₃, benzene, toluene, xylene, HCHO; ceilometer: MLH



Optical remote sensing:
[Ceilometer](#)
Vaisala LD40 or CL31
wave length: 855 or 910 nm
range: 4000 m
resolution: 10 or 7.5 m



Methodology



CUGB: PM_{4.3} (2010.06.21 – 2011.06.20)

IAP: PM_{2.5} (2013.04.10 – 2013.06.08)

ZBAA: Weather station

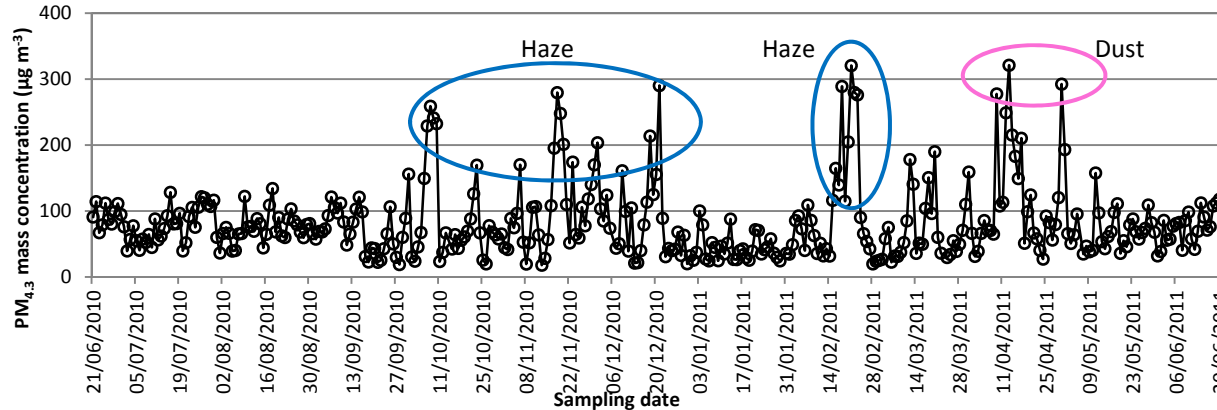


Methodology

- Samplers: 2 high volume samplers DHA-80 (500 l min^{-1})
- Filters: Quartz fiber filters ($\varnothing 150 \text{ mm}$)
- Sampling time: 24 h (00:00-24:00)
 4 h (some haze episodes, 2013)
- Use of filters:
 - Sampler A
 - ❖ Organic - Gas chromatography-mass spectrometry
 - ❖ EC/OC - Thermal/optical carbon analyzer
 - ❖ Ions - Ion chromatography and continuous flow analyzer
 - Sampler B
 - ❖ Mass concentration - Balance for gravimetric determination
 - TEOM (Tapered element oscillating microbalance)
 - ❖ Inorganic elements - Polarized energy dispersive X-ray fluorescence ($\text{PM}_{4.3}$)
 - Inductively coupled plasma mass spectrometry ($\text{PM}_{2.5}$)

Results - Variation

- PM_{4.3} mass concentrations (2010-2011)



Definition of seasons:

Spring: April – May

Summer: June – August

Autumn: September – October

Winter: November - March

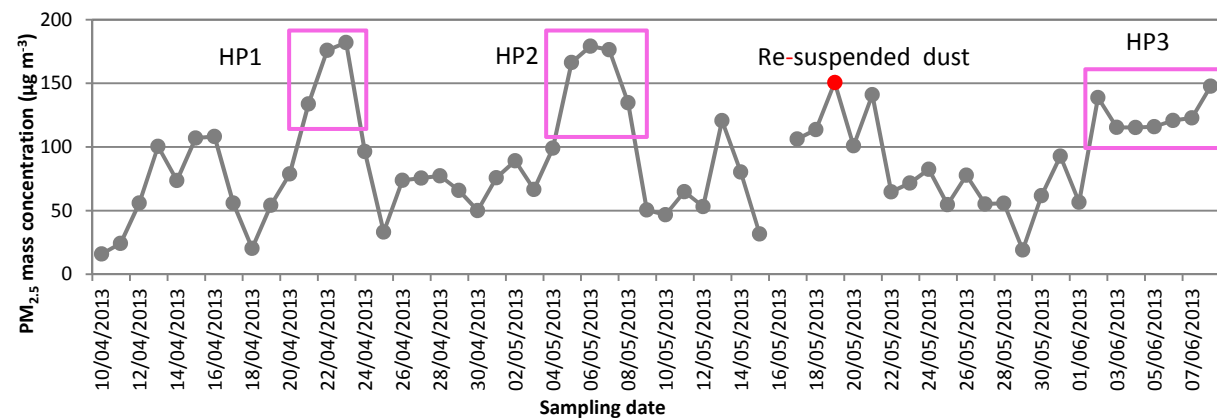
24 h PM_{2.5} threshold values:

WHO: 25 $\mu\text{g m}^{-3}$

US-EPA: 35 $\mu\text{g m}^{-3}$

China (Grade II): 75 $\mu\text{g m}^{-3}$

- PM_{2.5} mass concentrations (Spring 2013)



2010-2011 PM_{4.3}:

Annual average: 83 $\mu\text{g m}^{-3}$

Haze: 168 $\mu\text{g m}^{-3}$

Dust: 215 $\mu\text{g m}^{-3}$

Clear: 43 $\mu\text{g m}^{-3}$

Spring 2013 PM_{2.5}:

Average: 89 $\mu\text{g m}^{-3}$

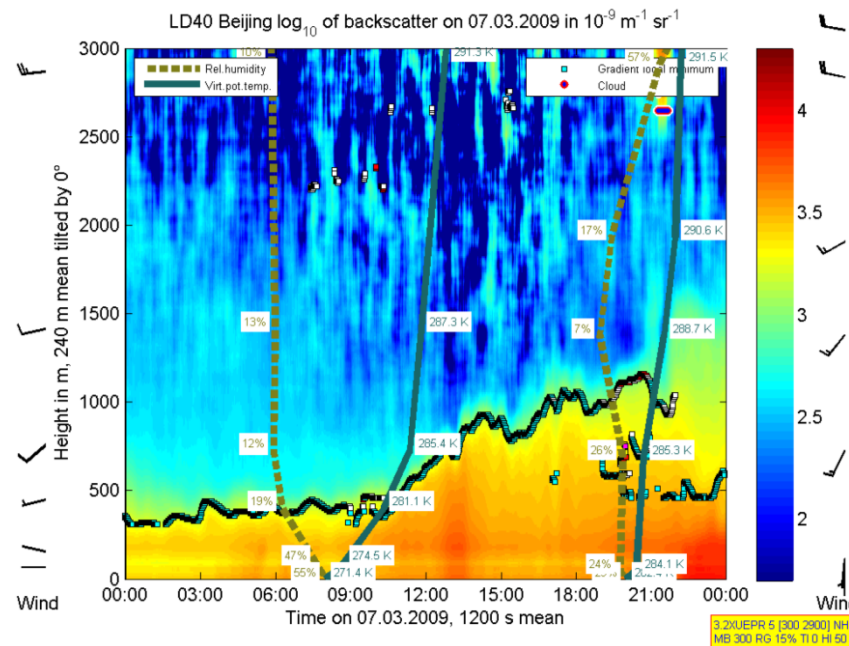
Haze: 140 $\mu\text{g m}^{-3}$

Dust: 125 $\mu\text{g m}^{-3}$

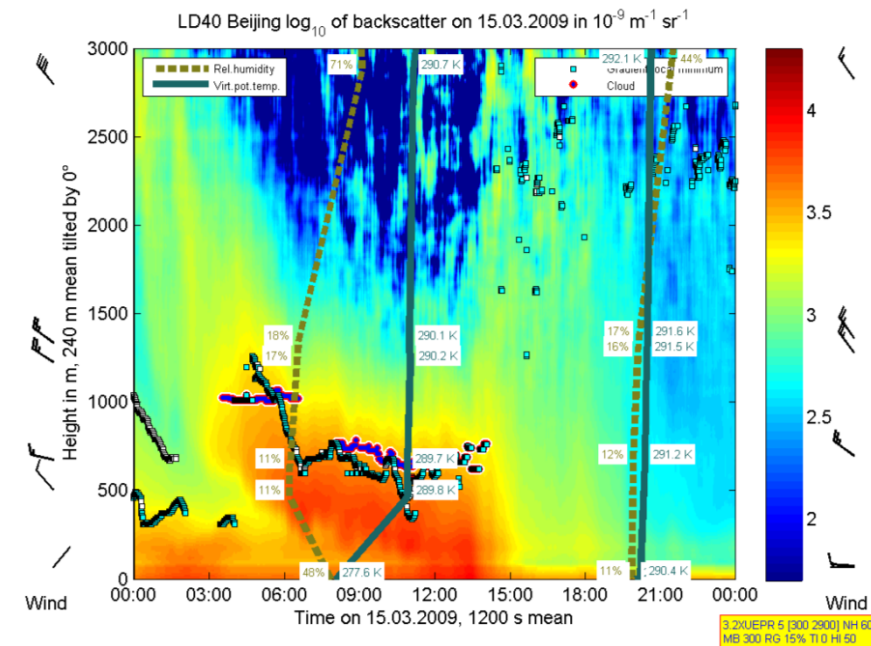
Clear: 45 $\mu\text{g m}^{-3}$

Evaluations

Higher particulate loads
during winds from South-West

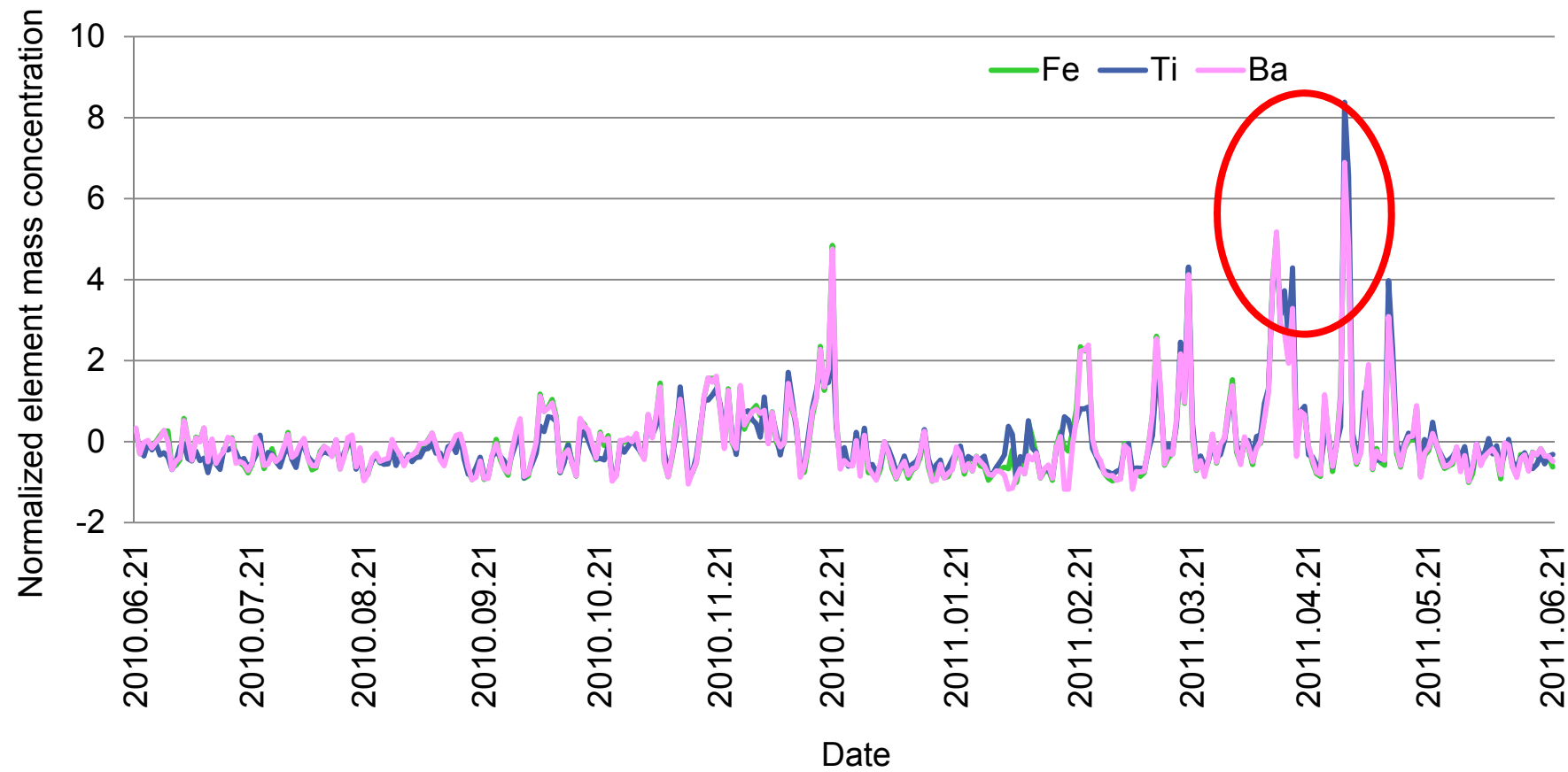


Desert dust clouds, winds
from West, dry air



MLH > 1000 m: often multiple layering, < 1000 m: often one layer
High PM_{2.5} load (40 – 140 µg/m³): MLH much lower than 1000 m

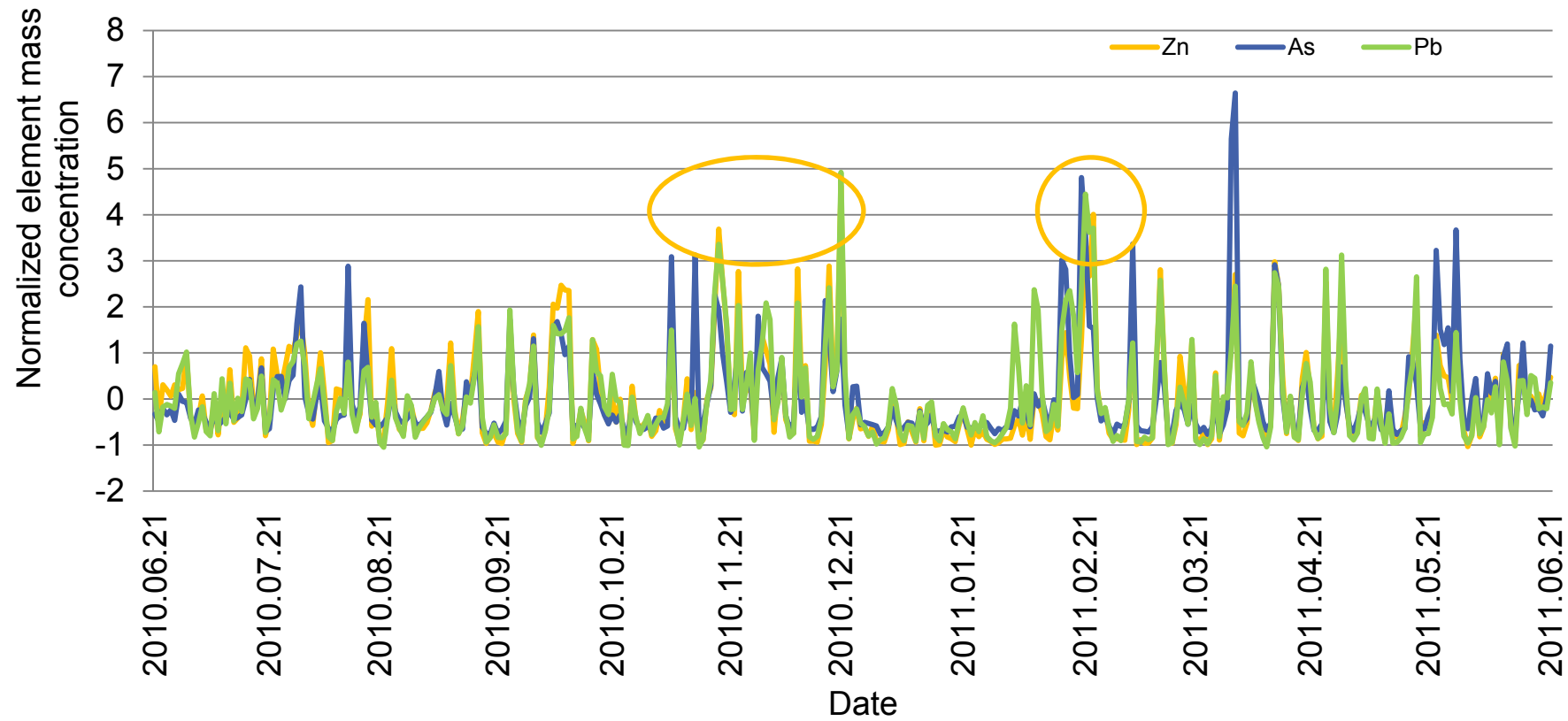
Variation of Fe, Ti and Ba



Highest in April because of dust storm (originated from Gobi desert) and re-suspended road dust

Dust events: different natural sources

Variation of Zn, As and Pb



Fossil fuel combustion (oil and coal combustion) and waste incineration, lowest in January - Spring Festival holidays

Haze days: highest PM mass concentration from anthropogenic activities, air pollution event during all seasons

Influence of MLH upon element mass concentrations

If the origin of the elements is

- the **soil** this source dominates the concentrations (Al, K and Ca no MLH influence),
- the **traffic and industry** the air transport dominates (no MLH influence in higher altitudes) and
- a **widespread area source** the MLH dominates (Cu, Zn)

Dust days: high wind speed

Meteorological influences



- RH: ↑ PM mass concentration
- WS: ↑ dilution of pollutants
- MLH: ↑ dilution of pollutants
- WD: transport pollution from local and regional

→ Haze days: high RH/low MLH, stagnant weather conditions with low air mass exchange

Visibility: negative correlated with RH and anthropogenic compounds, especially NO_3^- , SO_4^{2-} , and NH_4^+
very few dust events

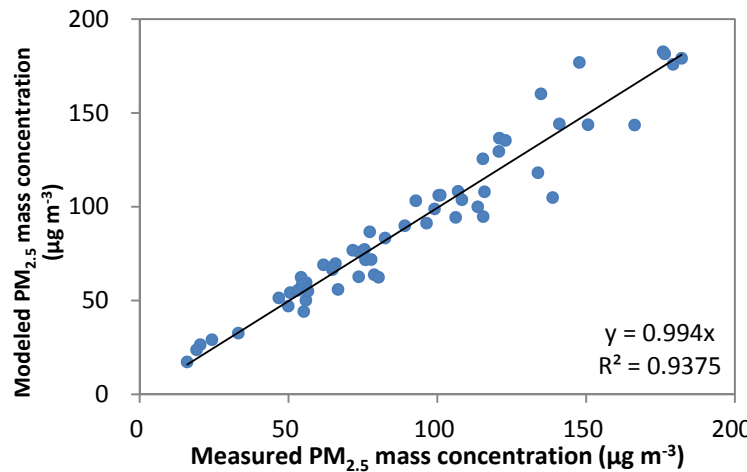
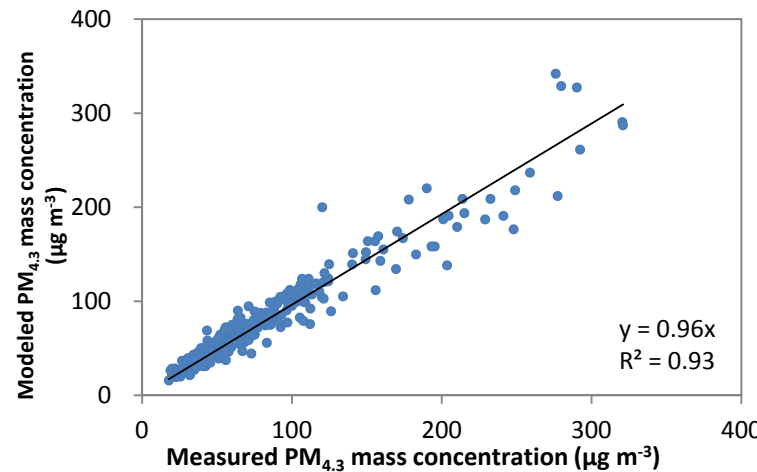
Discussion

- Wind conditions influence urban air quality -> contribution of surrounding emissions: e.g. source apportionment of PM_{2.5}
- MLH influenced by future climate change – quality of living in cities
- Only holistic and multidisciplinary approaches provide a deeper understanding -> measurements and modeling

Methodology – Source apportionment

- Positive matrix factorization (PMF)

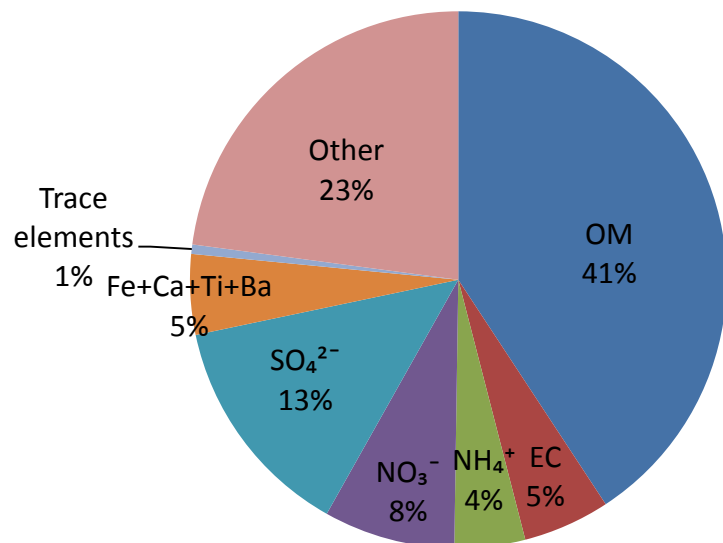
$$x_{ij} = \sum_{k=1}^p g_{ik} f_{kj} + e_{ij}$$



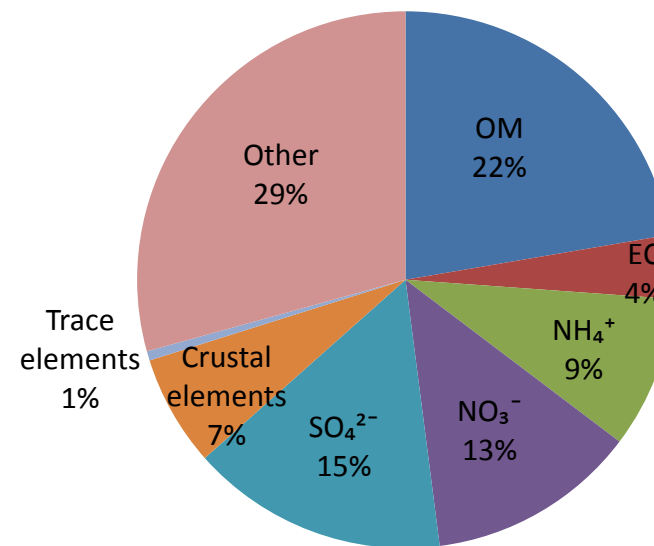
- Backward trajectory - HYSPLIT4 (Hybrid Single Particle Lagrangian Integrated Trajectory)
 - Height: 500 m at target point
 - Duration: 72 h

Results - Mass Balance

June 2010 – June 2011



April – June 2013



- June 2010 – June 2011, PM_{4.3}: 41% OM & 25% secondary inorganic ions
- April – June 2013, PM_{2.5}: 22% OM & 37% secondary inorganic ions

Results - Ratios Between Compounds

- Levoglucosan/OC → estimation of biomass burning contribution
- Hopane index: $30ab/(30ab+30ba)$ → vehicle exhaust emission or coal combustion source
 $17\alpha(H)21\beta(H)\text{-Hopane}/(17\alpha(H)21\beta(H)\text{-Hopane} + 17\beta(H)21\alpha(H)\text{-Hopane})$
- Homohopane index: $31abS/(31abS+31abR)$ → vehicle exhaust emission or coal combustion source
 $22S-17\alpha(H)21\beta(H)\text{-Homohopane}/(22S-17\alpha(H)21\beta(H)\text{-Homohopane} + 22R-17\alpha(H)21\beta(H)\text{-Homohopane})$
- BGH/BEP → vehicle exhaust emission source
 $\text{benz(g,h,i)perylene/benzo(e)pyrene}$
- IND/(IND+BGH) → vehicle exhaust emission or coal combustion source
 $\text{indeno(1,2,3,c,d) pyrene}/(\text{indeno(1,2,3,c,d) pyrene} + \text{benz(g,h,i)perylene})$
- Mg/Al → dust source from inside or outside Beijing

Haze 2010-2011:

Summer: Biomass burning and secondary inorganic ions

Autumn: Secondary inorganic ions

Winter: Coal combustion

Spring: Dust

Indicating sources of PM

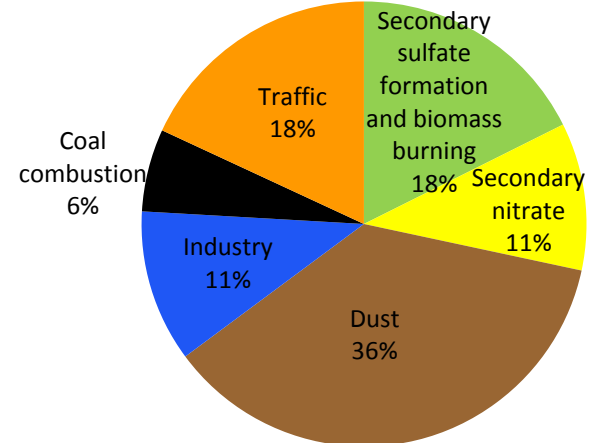
Results – PM_{2.5}/PM₁₀ (TEOM Data)



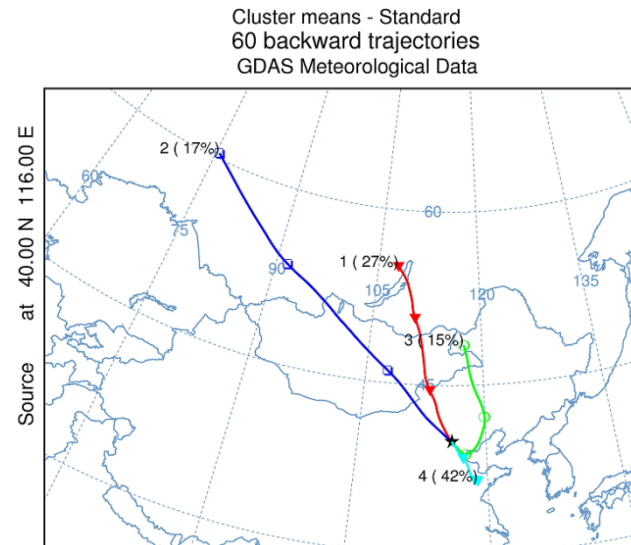
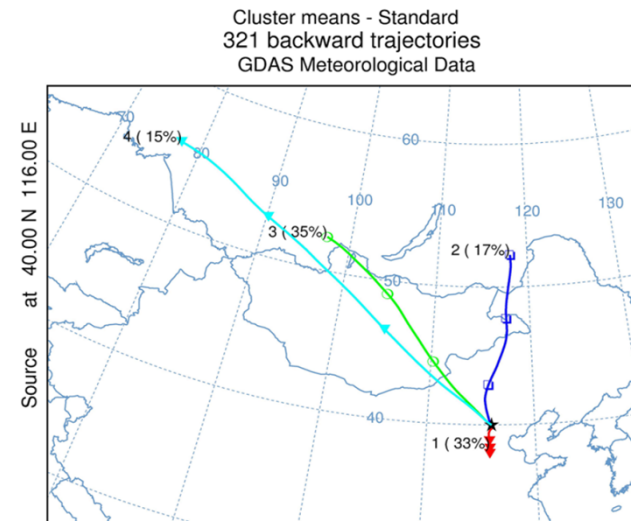
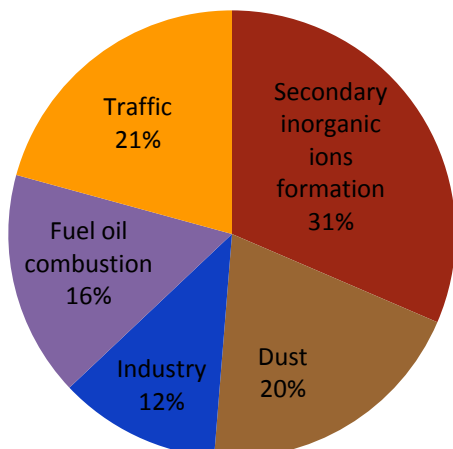
- 2010.06 – 2011.06
 - Haze: 0.55
 - Clear: 0.35
 - 2013.04 – 2013.06
 - Haze: 0.68
 - Dust: 0.25
 - Clear: 0.38
- Contribution of fine particles ↑ during haze

Results - Source Apportionment

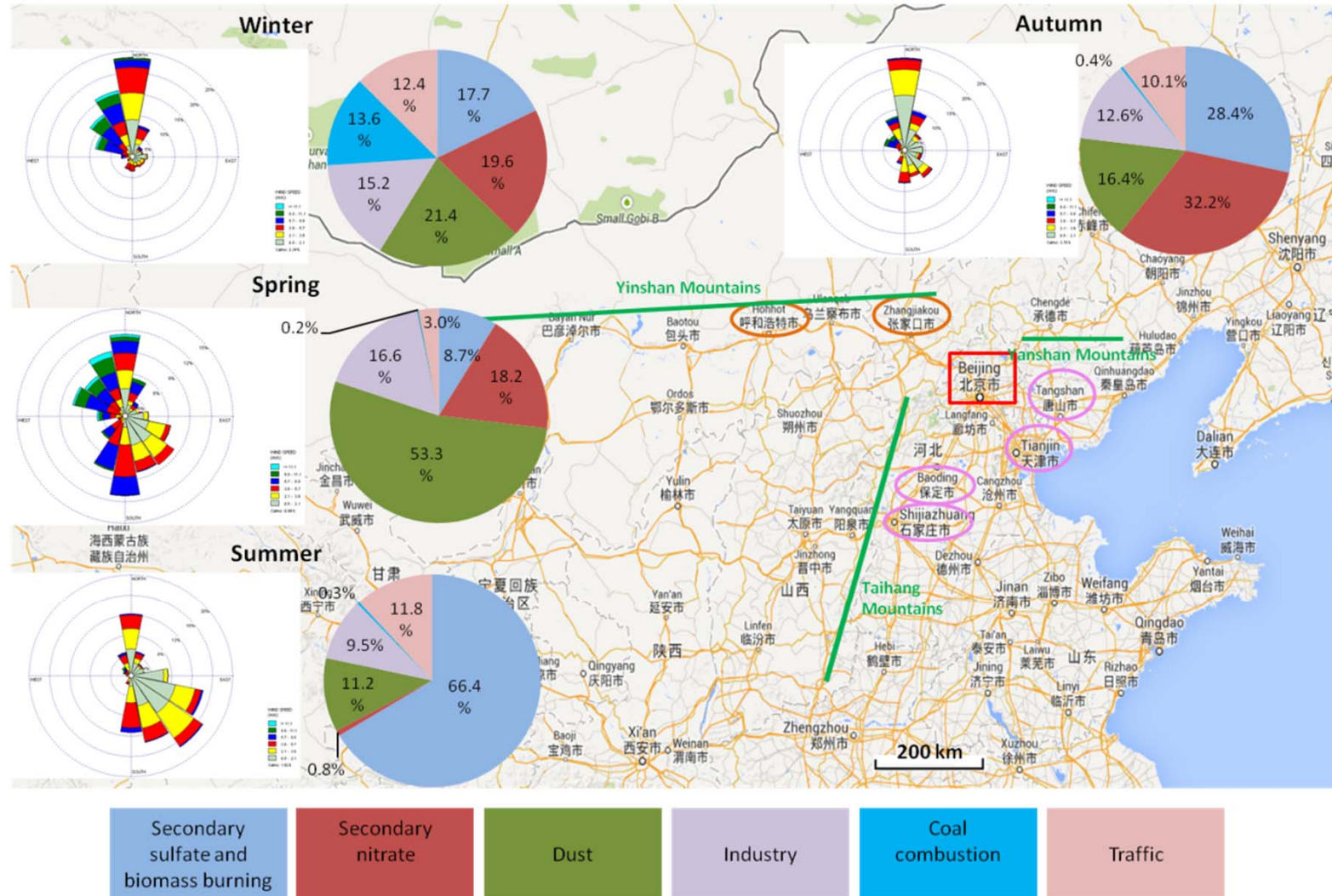
- June 2010 – June 2011



- April – June 2013



Summary – Orography, Meteorology and Emissions in the Surroundings



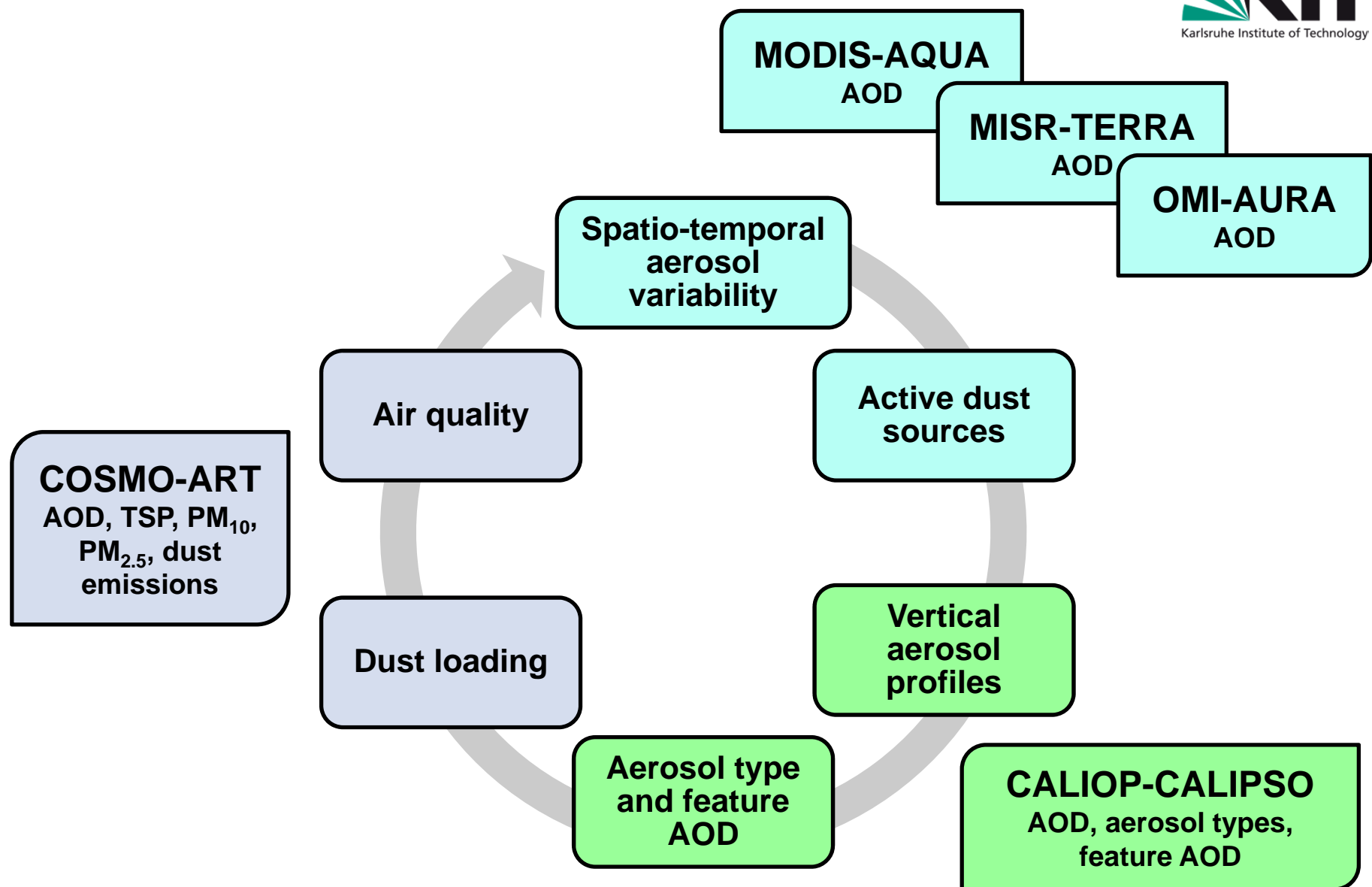
Conclusions

- PM mass concentrations after Olympic Summer Games 2008 are still high
- Haze becomes more frequent because an increasing number of fine and anthropogenic particles is emitted and stagnant weather conditions are not decreasing
- Haze in different seasons was caused by different sources and source regions due to different dominating transport conditions (local, regional and long-range as well as different directions) and regional air quality situation
- Controlling the emission of precursor gases of NO_3^- , SO_4^{2-} , and NH_4^+ in regional scale is necessary for reducing haze
- Installation of cleaning equipment in industrial exhaust and mobile vents, improving road cleaning standards and reducing construction dust also becomes important for improving air quality

Meteorological influences upon urban air quality

Mineral dust exposure in Beijing

Methodological approach



COSMO-ART

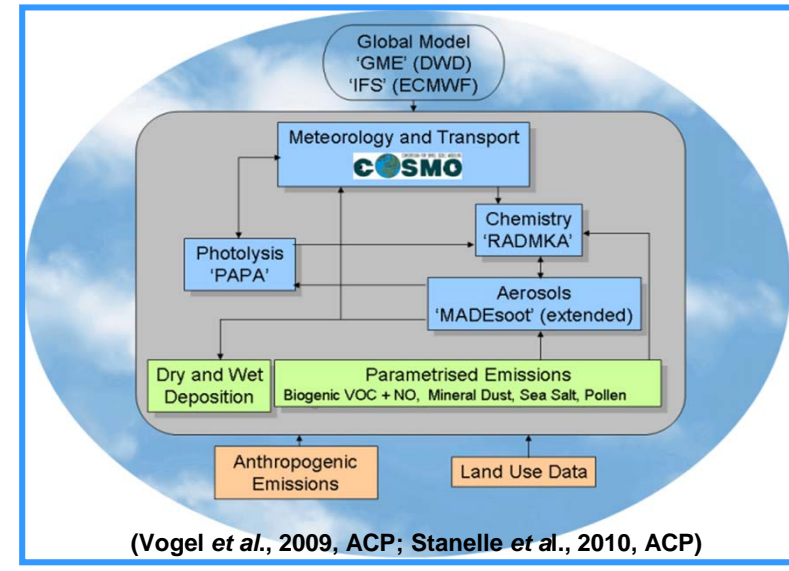
Aim: Investigation of impact of gases and aerosols on air quality (continental to local scales)

Gases & Aerosols: 80 gas species, 5 anthropogenic aerosol modes, **mineral dust**, sea salt, pollen

Feedbacks: meteorology, aerosols, gas phase, dynamics, clouds

Mineral dust:

- 3 initial dust modes, dust emissions, TSP, PM₁₀, PM_{2.5}, AOD
- Emissions: surface properties, friction velocity, soil moisture
- AOD: calculated online as function of extinction coefficients, single scattering albedo derived a priori according to dust size and number concentrations using Mie theory



(Vogel et al., 2009, ACP; Stanelle et al., 2010, ACP)

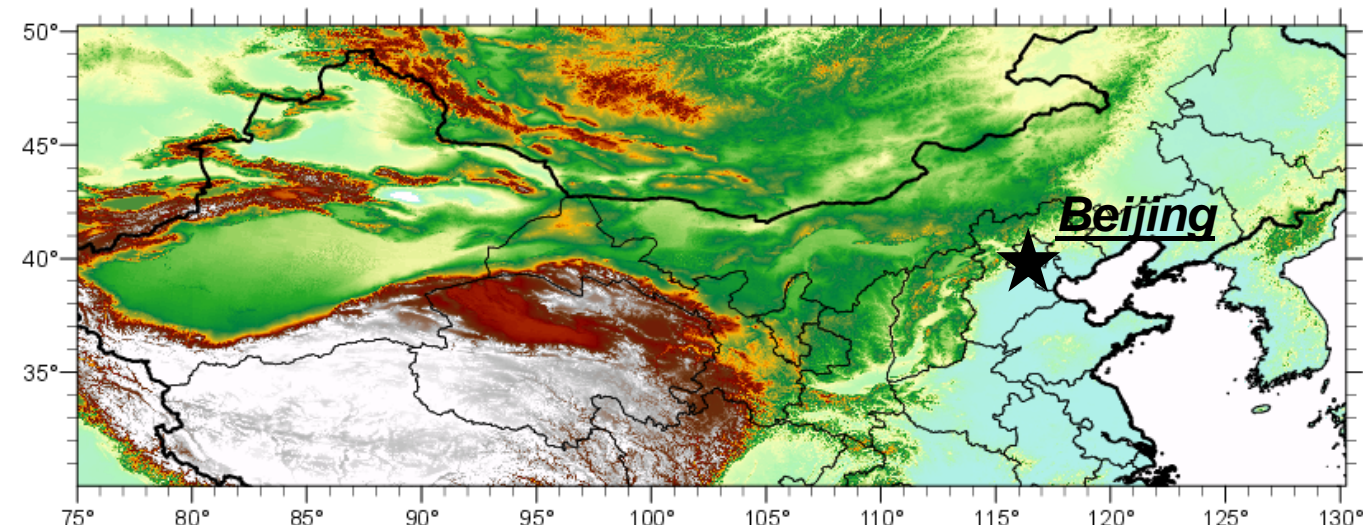
COSMO-ART
(Consortium for Meso-scale Modeling –
Aerosols and Reactive Trace Gases)

Data overview

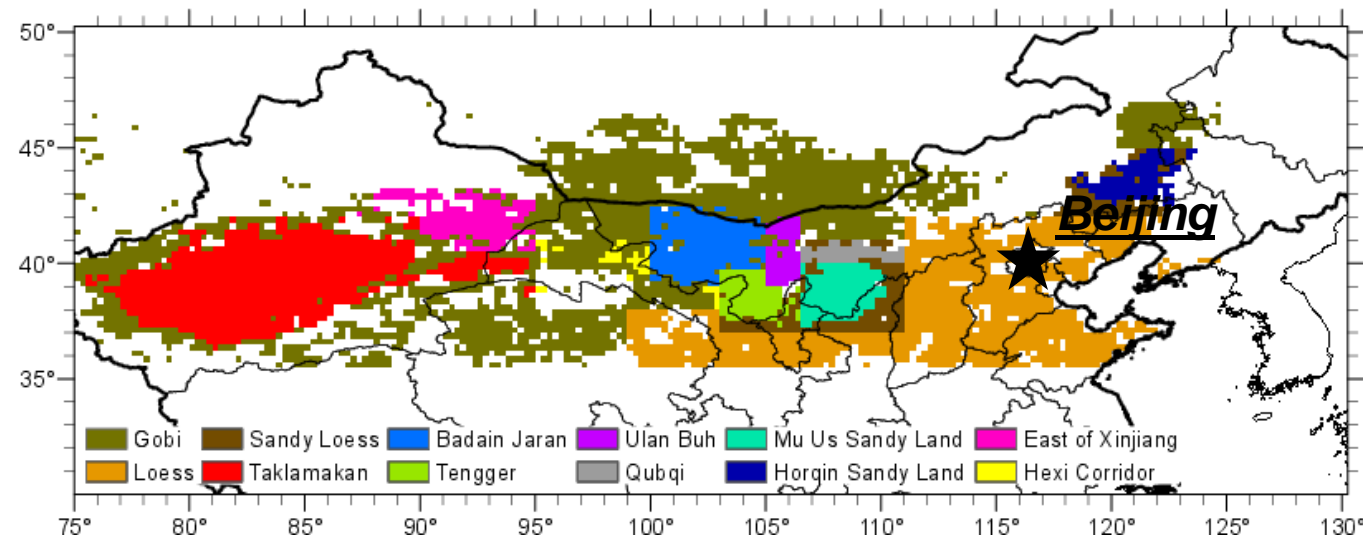
	Parameters and product	AOD wavelength	horizontal resolution	vertical resolution
MODIS	Deep Blue AOD Collection 5.1, Level 2	550 nm	10 x 10 km	-
OMI	Near-UV AOD OMAERUVd, Level 3	500 nm	1 x 1°	-
MISR	Green band AOD MIL2ASAE, Collection 11, Level 2	555 nm	0.15 x 0.15°	-
CALIOP	AOD, aerosol types Level 2, data version 3.01	532 nm, 1064 nm	5 x 5 km	333 m
COSMO-ART	AOD, TSP, PM ₁₀ , PM _{2.5} without anthropogenic emissions	555 nm	28 x 28 km	Varying terrain following layers

Study area and dust source regions

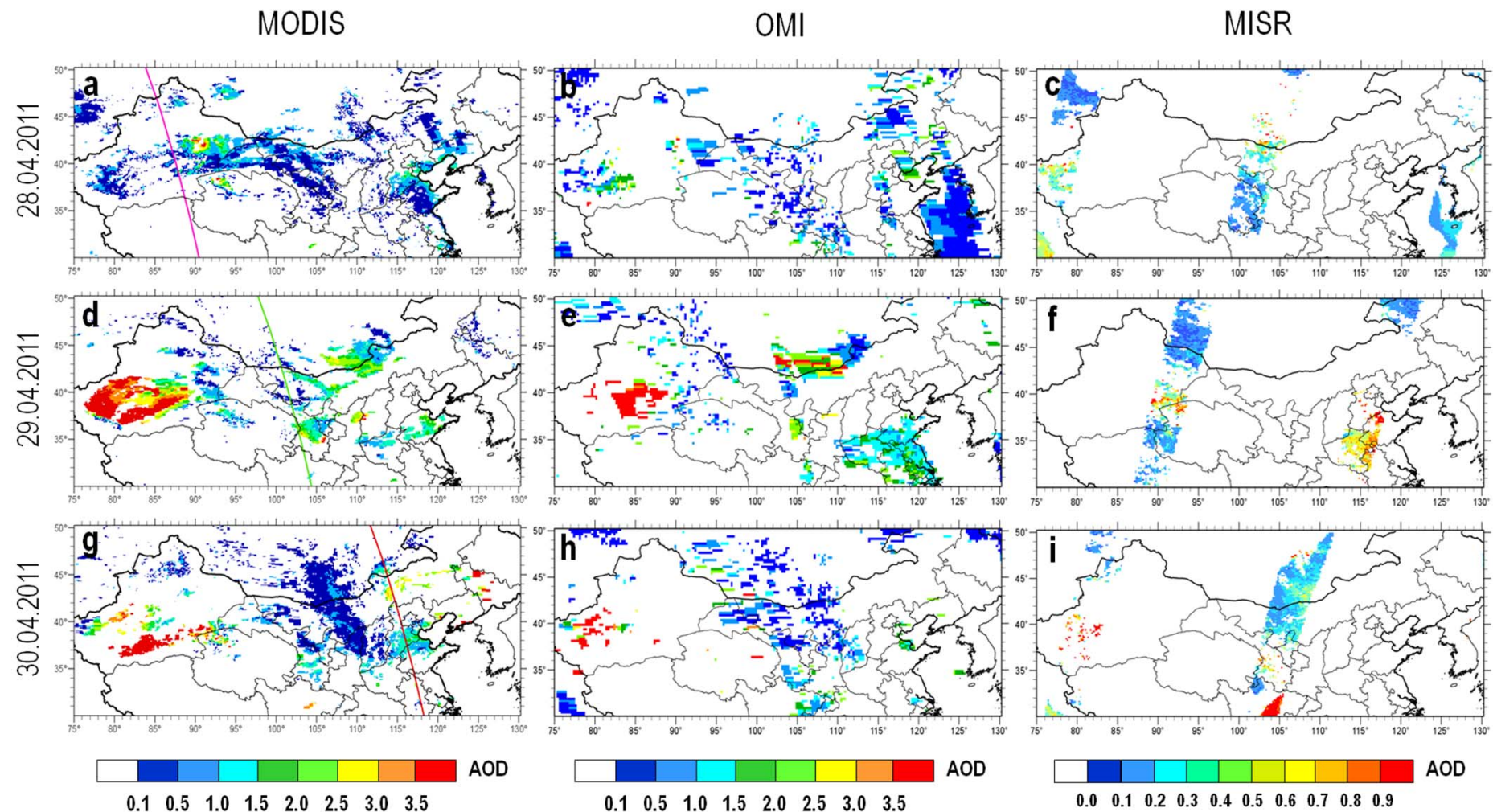
Model domain



Desert areas in
Northern China

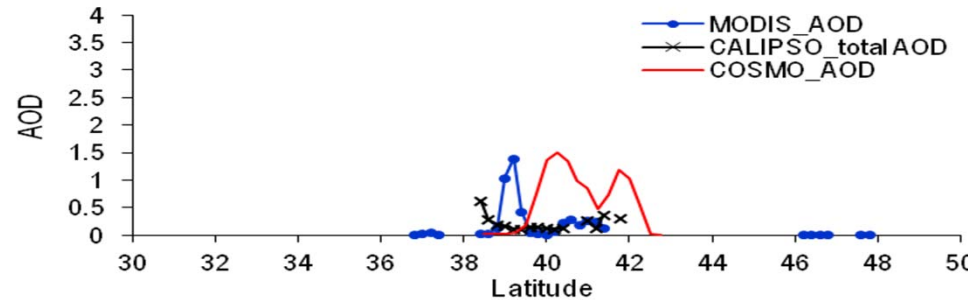


Spatio-temporal variability of AOD by passive sensors

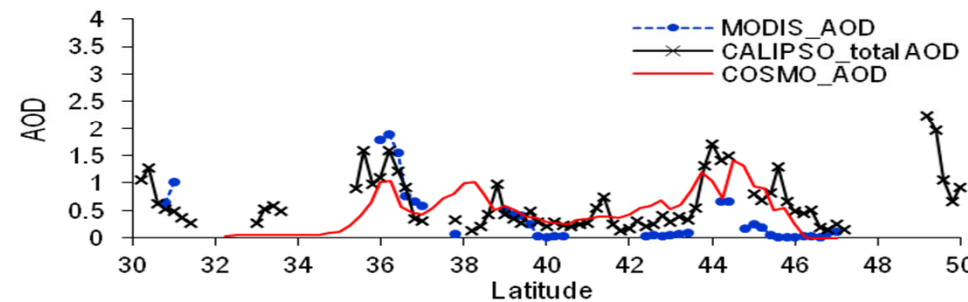


Satellite information for air quality modeling - AOD

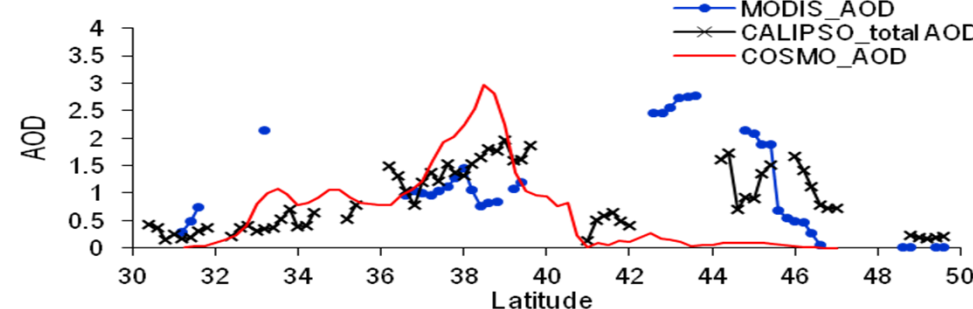
28.04.2011_07:30 UTC_Taklamakan Desert



29.04.2011_06:30 UTC_Central China



30.04.2011_05:30 UTC_Inner Mongolia/ Beijing

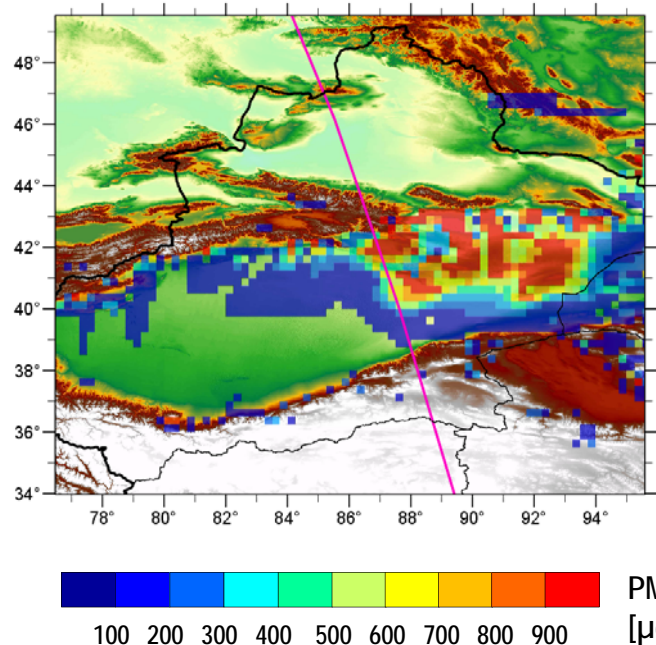


Comparison of measured AOD by MODIS and CALIPSO and simulated AOD by COSMO-ART for model validation

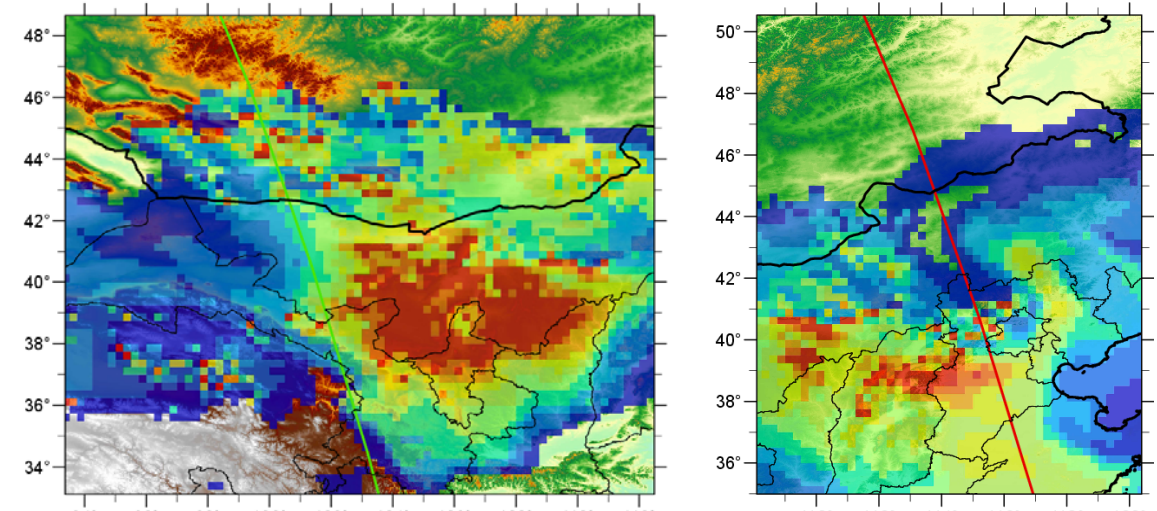
Impact of mineral dust on air quality – PM_{2.5}

Simulation of local PM_{2.5} mass concentrations

28/04/2011, 07:30 UTC
Taklamakan Desert

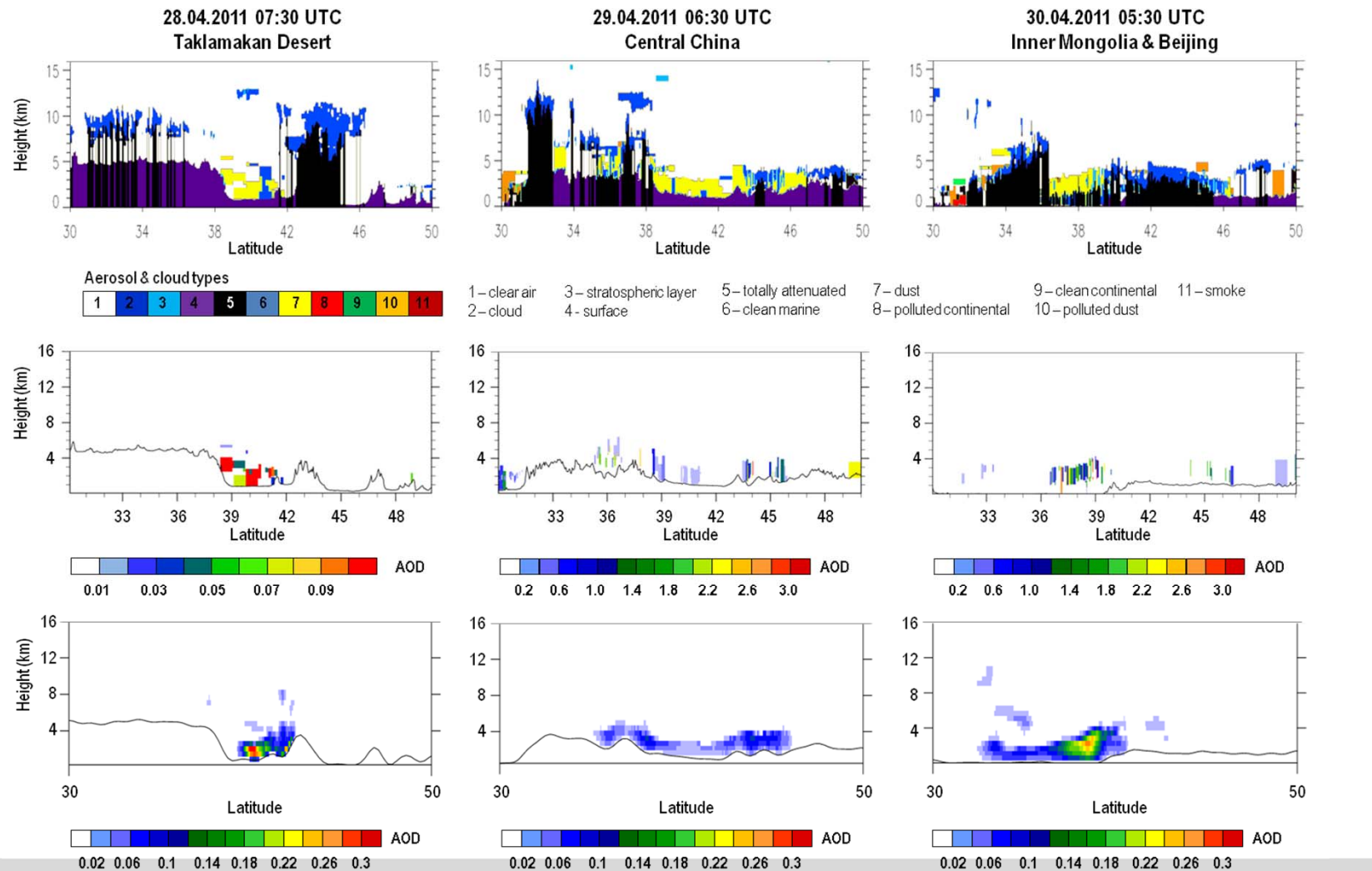


29/04/2011, 06:30 UTC 30/04/2011, 05:30 UTC
Central China Beijing & Inner Mongolia



Impact of mineral dust on air quality – AOD

Comparison of CALIPSO features and feature AOD and simulated COSMO-ART AOD



Conclusions

- Dust is present over most of the desert areas
→ main source regions Kumtaq, Taklamakan, Gobi
- Most mineral dust is located near the ground → air quality
- Good accordance aerosol by satellites and simulated dust
→ Space lidar and passive sensors - aerosol model validation
- We have to investigate
 - Traffic emissions and its development (e.g. UFP, BC)
 - Feedback mechanisms climate change & air quality
 - Consequences to human health: PM_{2.5}, PSD -> UFP
- Study future developments and recommendations relevant for decision makers and stakeholders to improve air quality and to limit climate change impacts

Acknowledgements

We like to thank for financial support within the frame of two start-up projects KIT centre Climate and Environment as well as State Baden-Württemberg, Helmholtz Graduate School for Climate and Environment (GRACE) at KIT and CSC for fellowships.

Thank you very
much for your
attention